Performance of Density Functionals for Calculating Barrier Heights of Chemical Reactions Relevant to Astrophysics

Stefan Andersson*,†,‡ and Myrta Grüning§

Leiden Observatory, P.O. Box 9513, 2300 RA Leiden, The Netherlands, Theoretical Chemistry, Leiden Institute of Chemistry, Leiden University, P.O. Box 9502, 2300 RA Leiden, The Netherlands, and Section Theoretical Chemistry, Vrije Universiteit, De Boelelaan 1083, 1081 HV Amsterdam, The Netherlands

Received: June 24, 2004

The performance of 39 different LDA, GGA, meta-GGA, and hybrid density functionals has been evaluated, for calculating forward and reverse barrier heights of 10 gas-phase reactions involving hydrogen. The reactions are all relevant to astrochemistry. Special focus is put on the applicability of DFT for calculating the rates of corresponding surface hydrogenation reactions that are relevant to the chemistry of ice-coated interstellar grains. General trends in the performance of the density functionals for reactions involving H atoms, H_2, and OH are discussed. The OH+CO reaction is shown to be a very problematic case for DFT. The best overall performance is found for the hybrid density functionals, such as MPW1K, B97-1, B97-2, and B1B95. For several reactions, the HCTH GGA functionals and the VS98 and OLAP3 meta-GGA functionals also give results that are almost as good as those of the hybrid functionals.

1. Introduction

Hydrogen is the most common element in the Universe, with an abundance that is at least a factor of 1000 higher than that of any carbon-, nitrogen-, or oxygen-bearing species. Thus, reactions with hydrogen, whether in atomic or molecular form, will dominate the chemistry in astrophysical situations if they can proceed rapidly. Many reactions of neutral molecules with hydrogen have small energy barriers, however, which cannot be overcome at the low temperatures ($T < 100$ K) prevalent in the interstellar gas. Only in high-temperature ($T \sim 2000$ K) shocked gas or on the surfaces of grains can these reactions occur within the lifetime of molecular clouds, of order 10 million years (for a general review see ref 1).

Despite the barriers to hydrogenation, several fully hydrogenated molecules have been widely detected in interstellar space, either as gas or as ice. Interstellar ices are observed in dense molecular clouds where the gas-phase species collide with the cold ($T \approx 10$K) silicate or carbonaceous grains and condense out to form icy mantles (see refs 2 and 3 for more extensive reviews). Hydrogen atoms or molecules are among the very few species that are mobile at these low temperatures, and they can diffuse over the surface and eventually react with an atom or molecule in the ice. CH_4, NH_3, and H_2O have also been detected and are believed to be formed through the successive addition of hydrogen to C, N, and O atoms at grain surfaces. Similarly, HCHO and CH_3OH, two important organic molecules, are thought to result from the successive hydrogenation of CO. Since the addition of H atoms to closed-shell species such as CO involve overcoming potential barriers,[4,5] tunneling must be involved to drive the reactions at thermal energies ($k_BT \approx 1$ meV at 10 K). The formation of HCHO and CH_3OH has been demonstrated experimentally by exposing a mixed H_2O−CO ice to a beam of H atoms at surface temperatures of 10−15 K.[5,6] For pure CO ices, similar experiments produced only small amounts of HCHO and no CH_3OH.[7,8] Experiments have also been performed for C_2H_2 and C_2H_4 ices, and in both these cases high yields of C_2H_6 were found.[7] During UV irradiation of water ice, H_2O molecules might be photodissociated and form energetic H and OH fragments. The reaction of an energetic OH radical with CO is a likely source of carbon dioxide. The interaction of H and OH with other species present in the ice is also a major concern for understanding the generation of many more complex organic species by this type of chemistry.

To understand the processes that occur on and in interstellar ice surfaces, computational studies will be essential, since the conditions in space are difficult or even impossible to mimic in the laboratory, especially the long time scales and low fluxes of atoms, molecules, and/or radiation. To calculate the rates of any of these processes, accurate estimates of their barriers in the presence of a surface are needed. Thus, an ice cluster or periodic slab of water molecules must be included in the model to fully describe the reaction. Although high level wave function-based ab initio methods, such as multireference configuration interaction (MRCI), can give reliable barriers and energetics for pure gas-phase reactions of astrophysical interest, they become computationally too demanding if a water cluster is added. Density Functional Theory (DFT) may be a time efficient alternative for studying these surface reactions.

In the Kohn−Sham[9] (KS) formulation of DFT, a reference system of noninteracting electrons moving in an effective potential is introduced. The central object in KS theory is the exchange-correlation energy, E_{xc}, which is a functional of electron density. This should contain all contributions to the energy that are not included in the simple Hartree approximation, i.e., it should cover the exchange energy, the correlation energy and a correction to the kinetic energy, to account for the difference in kinetic energy between the noninteracting and fully interacting systems. The exact KS theory yields the exact

* To whom correspondence should be addressed. E-mail: s.andersson@chem.leidenuniv.nl.
† Leiden Observatory.
‡ Leiden Institute of Chemistry.
§ Vrije Universiteit, Amsterdam. Present address: Donostia International Physics Center, E-20018 San Sebastián, Basque Country, Spain.

10.1021/jp040448c CCC: $27.50
Published on Web 08/19/2004

ground-state energy and density for N electrons subject to an external potential. In practice, the schemes for calculating E_{xc} are laid down in approximate density functionals, which often are formulated as separate contributions to E_x (exchange functionals) and E_c (correlation functionals). A host of approximate density functionals have been proposed (for example see refs 10 and 11).

The simplest density functional is the local (spin) density approximation (LDA, LSD or LSDA) where E_{xc} depends on local electron density only. It is usually constructed from the Slater−Dirac exchange[12,13] and VWN[14] correlation functionals. The next level of approximation is reached by introducing a gradient correction to the LDA, i.e., E_{xc} also depends on the gradient of the electron density. These functionals are referred to as generalized gradient approximation (GGA) functionals or GGAs. Popular GGAs include Becke's 1988 exchange functional[15] (B or B88x), which is often used together with Perdew's 1986 (P86) correlation functional[16] and the LYP correlation functional.[17] Together with the PW91,[18,19] PBE,[20] revPBE,[21] and RPBE[22] functionals they will be referred to as 'standard' GGAs. Further improvement can be reached if the density functional includes the (noninteracting) kinetic energy density and/or Laplacian of the electron density as parameters. These functionals are often referred to as meta-GGAs. Early examples include Becke's 1988 correlation functional[23] (B88c) and the Becke-Roussel 1989 exchange functional[24] (BR89x). By mixing in a portion of exact (Hartree−Fock type) exchange in the functional, one arrives at the hybrid functional scheme introduced by Becke.[25,26] The most popular hybrid functional to date is B3LYP.[26,27]

A major incentive for using DFT is its low computational cost, which is especially important for large systems. The computing time of Hartree−Fock (HF) calculations formally scale as N^4, where N is a measure of the size of the system (e.g. the number of electrons or basis functions). Post-Hartree−Fock methods including electron correlation have a more unfavorable scaling. Møller−Plesset second-order perturbation theory (MP2) scales as N^5 and the highly accurate CCSD(T) (coupled-cluster (CC) with single and double excitations and a perturbative treatment of triple excitations) method as N^7. Hybrid density functionals basically have the same scaling as Hartree−Fock, while the nonhybrid functionals all have a more favorable scaling (about N^3) with system size. It should be noted that there are algorithms available that give much more favorable scaling for large systems. For extended molecules and clusters, even linear scaling (proportional to N) has been achieved for DFT, HF, MP2, and CC methods (see refs 28−32 and references therein). There is of course much to be gained in using methods that are as computationally cheap as, or cheaper than, Hartree−Fock, but that have a much higher accuracy.

In contrast to ab initio theory, where it is very well-known how to improve results (going toward the full correlation (full configuration interaction) and complete basis set limits) and the only major issue is the computational effort, in DFT the development of approximate exchange-correlation functionals is a matter of ongoing research. A relatively large number of approximate functionals have been developed in the last two decades, both in a 'semiempirical' fashion, fitting some parameters of the functional to a set of reference data, and also in a more systematic way, trying to satisfy exact constraints.[33−35] Thus, the use of approximate density functionals requires great care, and there is not, to the best of our knowledge, a functional that gives a universally accurate description of molecules *and* surfaces, including equilibrium geometries, reaction barrier heights, intermolecular interactions, and surface adsorption energies. Careful testing of the performance of density functionals is thus needed for a number of model systems, to ascertain the applicability of a certain functional to specific problems, such as reactions involving hydrogen.

There have been a number of publications reporting the performance of density functionals in predicting barrier heights of gas-phase chemical reactions.[36−85] Early on, it was recognized that the LDA was totally unreliable,[37−41] underestimating barrier heights by 0.5−1.0 eV for reactions involving the transfer of hydrogen atoms. In the same studies, it was also shown that using gradient-corrected density functionals, such as BP86, BLYP, and PW91, in many cases gave a clear improvement in barrier heights, leading to results that were at least qualitatively correct and of comparable accuracy to post-Hartree−Fock methods, such as MP2. With the standard GGAs, there still is a systematic underestimate of barrier heights in contrast to ab initio methods, which tend to overestimate barriers.

With the advent of hybrid functionals it was found that reaction barriers could be even better described than with the GGAs.[42−51] Hybrid functionals with a large amount of exact exchange (40−60%), such as BHandHLYP,[42−45] MPW1K,[52−54] and KMLYP,[57] have been reported to give good values for barrier heights in a variety of hydrogen abstraction and hydrogen addition reactions. Some hybrid functionals with a modest amount of exact exchange (20−30%) have also shown good performance for reactions involving hydrogen atoms or proton transfer. These include B97-1,[58,59] B97-2,[59,60] and B1B95.[61−63] Recently, GGA (HCTH/93[58]) and meta-GGA (FT98,[64] VS98 (VSXC),[61,62] BLAP3,[63] and Bmτ1[63]) density functionals have been devised that give barrier heights that are almost as good as those calculated with the best hybrid functionals.

The tendency of many density functionals to underestimate potential barriers can be attributed to the problem of *self-interaction*,[65] i.e., an unphysical interaction of an electron with its own charge distribution. There have been a few studies that have applied the *self-interaction correction* (SIC) scheme proposed by Perdew and Zunger.[86] Johnson and co-workers[65,66] studied the $H+H_2$ reaction and found that the use of self-interaction corrected functionals led to a dramatic increase in barrier heights. These barrier were both qualitatively and quantitatively better than for (uncorrected) LDA, GGA, and hybrid functionals. In a more recent study[67] other reactions were studied, e.g., hydrogen abstraction and S_N2 reactions, showing that applying SIC led to a considerable increase in barrier heights compared to LDA and revPBE results. However, bond lengths are rather severely underestimated[87] using SIC and there is no clear improvement in reaction energies.[67,87] Moreover, SIC calculations involve a higher computational effort, and as explained later in section 3A, applying SIC seems in many cases redundant for practical applications, as it corrects for wanted and unwanted features alike and even more so because of the high computational effort involved (see also refs 88−90).

The work that we present in this paper serves two main goals. First, we wish to study the performance of density functionals for predicting barrier heights of gas-phase reactions involving hydrogen. Second, as the corresponding *surface* reactions are important for understanding the chemistry of interstellar ices, these calculations serve as a first step in assessing density functionals for use in simulations of such surface processes. For the surface reactions, there are very few high-level ab initio calculations to compare with (an exception being ref 4). Clearly, the next step will necessarily be to assess the performance of

TABLE 1: Classical Barrier Heights and Reaction Energies of the Reference Energetics (in eV)

reaction	forward barrier	reverse barrier	reaction energy	geometry optimization	energetics
$H+CO \rightarrow HCO$	0.132	0.977	−0.845	MRCI+Q/cc-pVQZ (ref 94)	FCC/CBS[a]
$H+HCHO \rightarrow CH_3O$	0.168	1.276	−1.108	RCCSD(T)/TZ2P(f,d) (ref 95)	FCC/CBS[b]
$H+C_2H_2 \rightarrow C_2H_3$	0.203	1.933	−1.730	POL-CI/modified Dunning−Huzinaga DZ (ref 96)	FCC/CBS[a]
$H+C_2H_2 \rightarrow C_2H_5$	0.096	1.846	−1.750	QCISD/6-311G(d,p) (ref 97)	CCSD(T)/aug-cc-pVTZ
$C(^3P)+H_2 \rightarrow CH+H$	1.280	0.119	1.160	MRCI+Q/cc-pVTZ (ref 98)	MRCI+Q/cc-pVTZ
$N(^4S)+H_2 \rightarrow NH+H$	1.243	0.094	1.149	NH and saddle point: QCISD/cc-pVDZ (ref 99) H_2: CCSD(T)/aug-cc-pVQZ (This work)	FCC/CBS[a]
$S(^3P)+H_2 \rightarrow SH+H$	1.024	0.067	0.956	MRCI+Q/cc-pVTZ (ref 100) H_2: CCSD(T)/aug-cc-pVQZ (This work)	FCC/CBS[a]
$CH_2+H_2 \rightarrow CH_3+H$	0.346	0.675	−0.330	saddle point: CISD/modified Dunning−Huzinaga DZ (ref 103) stable species: CCSD(T)/aug-cc-pVQZ (This work)	FCC/CBS[a]
$OH+O \rightarrow H+CO_2$	0.112[c]	1.096[c]	−1.024	CCSD(T)/cc-pVTZ (ref 104)	FCC/CBS[b]
$H+H_2O \rightarrow H_3O$	0.885	0.099	0.786	CCSD(T)/aug-cc-pV5Z (ref 105)	FCC/CBS[a]

[a] Extrapolated from CCSD(T)/aug-cc-pVTZ and aug-cc-pVQZ. [b] Extrapolated from CCSD(T)/cc-pVTZ and cc-pVQZ. [c] OH+CO forward and reverse barriers do not correspond to the same stationary point (see the text for details).

density functionals for intermolecular interactions, before making the full surface calculations.

We have performed DFT calculations on classical barrier heights (excluding zero-point energies) and reaction energies (endo- or exoergicities excluding zero-point energies) for 10 systems. Of these, four are of the type

$$H + X \rightleftharpoons HX \ (X = CO, HCHO, C_2H_2, C_2H_4)$$

where the forward reaction is an exothermic *hydrogen addition* reaction and the reverse reaction can be classified as *unimolecular dissociation*. As discussed above, the hydrogen addition reactions, when occurring on a surface, could be a major source of hydrogenated organic molecules. Jursic[68,69] has previously studied the $H+C_2H_4$ and H+CO reactions using DFT. Additionally, four systems are of the form

$$X + H_2 \rightleftharpoons XH + H \ (X = C, N, S, CH_2)$$

where both the forward and reverse reactions are *hydrogen abstraction reactions*. These systems will be referred to as the XH_2 systems. The forward reactions, which all involve substantial barriers, can be a source of hydrogenated molecules in shocked interstellar gas. The reverse XH+H reactions are not only possible sources of 'dehydrogenation' in the same environments, but can also be competing with (barrierless) hydrogenation reactions on surfaces. The two final systems are

$$OH + CO \rightleftharpoons H+CO_2$$

and

$$H + H_2O \rightleftharpoons H_3O$$

The former, most often referred to as the *HOCO system*, involves the formation of a complex, which makes it quite distinct from the other systems where reaction passes through a single barrier, i.e., a direct process. The forward reaction may be one source of CO_2, which has been observed in interstellar ices, with OH possibly coming from a photodissociated H_2O molecule (see for instance ref 91) or appearing from the gas phase.[92,93] The $H+H_2O$ reaction involves the formation of a metastable H_3O species, which is a local minimum on the potential energy surface, but whose energy is above the $H+H_2O$ asymptote. This latter reaction is included to get an idea of how well approximate density functionals are expected to treat the interaction of hydrogen atoms with H_2O ice surfaces.

The remainder of this paper is organized as follows. In section 2 the density functionals and basis sets that have been used are discussed. Section 3 begins with a discussion of the problems and possible improvements of approximate density functionals for 'difficult' molecular systems. Then the results are discussed, starting with the overall performance for all the reactions, further considering specific classes of reactions and ending with accounts of how sensitive the results are to geometry optimization and the choice of basis sets. In section 4 some conclusions are presented, with particular reference to the applicability of the density functionals used in this work to the types of systems studied.

2. Computational Details

As was discussed in the Introduction, we have studied 20 barriers (forward and reverse) and 10 reaction energies. DFT calculations were performed using ab initio geometries taken from the references indicated in Table 1, with the exception of the CH_2+H_2 reaction where the geometries of the stable species were reoptimized as described below. The atomization energies presented in section 3E were calculated using MP2 geometries. Here the reference energies (excluding zero-point energies) were taken from ref 106. We also made additional geometry optimizations for the H+CO reaction, which are discussed separately in section 3H. Our results have been validated against the set of reference energetics (in eV) summarized in Table 1 (reference energies in kcal mol^{-1} can be found in the Supporting Information). When calculating the errors in the reaction energies, all reference energies have been taken to be positive (i.e. endoergic). The reference energies have been calculated following a scheme proposed by Yu et al.[104] They combined an extrapolation scheme to achieve the complete basis set (CBS) limit for the electron correlation energy, devised by Halkier et al.,[107] with a correction for the incomplete account of electron correlation in CCSD(T) calculations. The following expression has been used in this work for the full coupled cluster/complete basis set (FCC/CBS) energy:

$$E_{\mathrm{FCC/CBS}} = E_{\mathrm{CCSD(T)/Q}} + \frac{27}{37}[E_{\mathrm{CCSD(T)/Q}} - E_{\mathrm{CCSD(T)/T}}] + \frac{1}{5}E^{\mathrm{T}}_{\mathrm{CCSD(T)/T}}$$

$E_{\mathrm{CCSD(T)/X}}$ is the correlation energy from a CCSD(T) calculation using basis set X = T, Q, where T and Q stand for the cc-pVTZ and cc-pVQZ,[108] or aug-cc-pVTZ and aug-cc-pVQZ[109] basis sets, respectively. $E^{\mathrm{T}}_{\mathrm{CCSD(T)/T}}$ is the perturbational energy of the triples excitation using a T basis set. The factor 1/5 has

been set to account for the fact that this term only accounts for 75−80% of the full triple- and higher-order contributions to the correlation energy.[104,110] Because of the inadequacy of coupled-cluster calculations to describe the $C+H_2$ saddle point (due to a strong multiconfigurational character of the wave function), the original MRCI+Q energies were used for this system. Almost all geometries have been taken from ab initio calculations reported in the literature (see Table 1). For the CH_2+H_2 system all stable species, i.e., excluding the saddle point, were geometry optimized with coupled cluster (CCSD-(T)) calculations with the aug-cc-pVQZ basis set. The saddle point geometry was taken from configuration interaction (CISD) calculations using a double-ζ basis set.[103]

The H_2 and CO molecule appear in more than one reaction. For the sake of consistency, their bond lengths have been taken to be the same for all reactions (0.742 Å for H_2 and 1.1322 Å for CO). The coupled-cluster calculations were performed with the Gaussian 03 program package.[111] The geometries that have been used in our calculations can be found in the Supporting Information.

On the basis of convergence tests using larger basis sets and considering possible errors in the correction for higher-order correlation, we believe that the reference energies, with one exception, are correct to within chemical accuracy (1 kcal mol^{-1} or 0.043 eV), given the fixed geometries. The reference energies for the systems with only one heavy atom, except $C+H_2$, can even be taken to be correct to within 0.5 kcal mol^{-1} (0.02 eV). The uncertainty in the accuracy then of course increases with system size. Because no extrapolation to the CBS limit was performed for the $C+H_2$ reaction, the reaction energy (and the $C+H_2$ barrier) could be in error by up to 2 kcal mol^{-1} (0.087 eV). The smaller (CH+H) barrier should, however, be of chemical accuracy, based on test calculations and comparison with the other XH_2 systems studied here.

We have performed calculations using 39 different density functionals, including LDA, GGAs, meta-GGAs, and 'low-exact exchange' hybrid and 'high-exact exchange' hybrid functionals. LDA is the standard combination of Slater−Dirac (S) exchange[12,13] and VWN correlation.[14] Becke's 1988 GGA exchange functional[15] (B88x) has been combined with the GGA correlation functionals P86,[16] LYP,[17] and OP[112] to form BP86, BLYP, and BOP, and with the meta-GGA LAP3 correlation functional[113] in BLAP3. In a modified form, B88x is also used in Bmτ1 together with the meta-GGA τ1 correlation functional.[63] The OPTX exchange functional by Handy and Cohen[114] has been used together with LYP and LAP3 to form OLYP and OLAP3. The latter was first proposed in the recent work by Grüning et al.[70] In mPWPW91, a modified version of the exchange functional of PW91, mPW,[115] is used together with the original PW91 correlation functional.[18,19] The other GGA functionals that have been used are PW91, PBE,[19,20] revPBE,[21] RPBE,[22] FT97,[116] HCTH/93,[58] HCTH/120,[117] HCTH/147,[117] and HCTH/407.[118] The HCTH/N functionals have 15 linear parameters that have been fitted, respectively, to training sets of $N =$ 93, 120, 147, and 407 atomic and molecular systems (including energy gradients).[58,117,118]

Functionals where both exchange and correlation are of a meta-GGA form are VS98 (VSXC),[61] KCIS-orig,[119] KCIS-mod,[119] PKZB,[120] PKZBx-KCISc,[119,120] BR89x−B88c,[23,24,121] and Becke00.[121] The difference between KCIS-orig, KCIS-mod, and PKZBx-KCISc is that the first two functionals include *modified* versions of PKZB exchange together with the KCIS correlation functional, while in PKZBx-KCISc the original exchange functional is used. The modified versions of the PKZBx have different values for the parameter D in eq 9 of ref 120. In KCIS-orig, $D = 0.101$, and in KCIS-mod, $D = 0.128$. Becke00 uses a modified form of the Becke−Roussel exchange functional[24] (BR89x) together with Becke's 1988 correlation functional[23] (B88c). The construction of VS98 involved fitting 21 parameters to a training set of molecular systems.[61]

Of the 14 hybrid functionals employed, eight are of the 'low-exact exchange' type, having about 20−30% exact exchange, i.e., B3LYP[26,27] (20%), B1B95-25[111] (25%), B1B95-28[122] (28%), mPW1PW91[115] (25%), PBE1PBE (PBE0)[123−125](25%), B98[126] (19.85%), B97-1[58] (21%), and B97-2[59] (21%). The two versions of B1B95 differ only in the amount of exact exchange. B1B95-25 is the default in Gaussian 03, while B1B95-28 is the original version with 28% exact exchange as recommended by Becke.[122] B1B95 and B98 are both examples of hybrid functionals where the correlation functional is a meta-GGA. We have also used six, 'high-exact exchange' functionals, which contain 40−60% exact exchange: BHandHLYP[15,17,25] (50%), MPW1K (MPW428)[52] (42.8%), MPW58[71] (58%), MPW60[71] (60%), KMLYP[57] (55.7%), and KMLYP-mod (55.7%). The MPW1K functional was obtained by reoptimizing the amount of exact exchange in mPW1PW91 against a test set of 20 hydrogen abstraction systems.[52] The same procedure was used for MPW58 and MPW60, but in this case only one barrier ($CH_4+H \rightarrow CH_3+H_2$) was used to calibrate the methods.[71] MPW1K, MPW58 and MPW60 will henceforth be referred to collectively as MPWX.

The KMLYP-mod functional was constructed during the course of this work. The difference from the original KMLYP is the amount of VWN correlation, which was decreased from 1.0 to 0.552. We found that KMLYP-mod gave quite good results for barrier heights (see section 3). Compared to the original KMLYP however it gives poorer *absolute* energies. For instance the electron affinities of O and F calculated by KMLYP-mod give deviations from experimental values by about 0.9 eV, whereas KMLYP gives errors of 0.05 and 0.13 eV.

We have used two program packages for our calculations. For the LDA, GGA (except mPWPW91) and meta-GGA functionals we employed a developer's version of the Amsterdam Density Functional (ADF) program package[127] and for mPWPW91 and the hybrid functionals we used Gaussian 03. The atomic basis functions in ADF are Slater type orbitals. For the fixed geometry calculations we used ZORA/QZ4P, a valence quadruple-ζ basis set with four polarization functions originally constructed for relativistic calculations, and for our calculations optimizing barriers for the H+CO reaction ET/QZ3P was used, an even-tempered quadruple-ζ basis set with three polarization functions. In ADF, the electronic densities have been optimized with BLYP and the rest of the functionals have then been evaluated using the BLYP densities. As mentioned in the paper by Grüning et al.[70] this is expected to introduce an error of a few tenths of a kcal mol^{-1} (about 0.01−0.02 eV). In Gaussian 03 the atomic basis functions are Gaussian-type orbitals. For the fixed geometry calculations we used the aug-cc-pVQZ basis set and for the H+CO geometry optimizations we used aug-cc-pVTZ for optimizing the geometries and aug-cc-pVQZ for the final energy calculation. In Gaussian 03, all density functionals have been used to optimize the electron density, i.e., the calculations have been performed self-consistently. Additional calculations have been performed using basis sets of double- and triple-ζ quality as discussed in section 3I. In ADF the DZP and TZ2P basis sets were used. In Gaussian 03 the 6-31+G(d,p) and 6-311+G(3df,2p) basis sets were employed.

The reason for using the very large quadruple-ζ basis sets is to ensure that energies are as close to the basis-set convergence limit as possible. It was pointed out in a recent paper by Boese et al.[128] that the correlation-consistent basis sets might not be the optimal choice for DFT calculations. However, the differences were small compared to other basis sets of similar size and also dependent on the functional that was used. The most important consideration for calculating relative energies using DFT is the use of diffuse basis functions, as was stressed by Lynch et al.[129] The effect of adding diffuse functions to a basis set will of course be different for different systems. For instance H_3O has an electron density that extends far from the nuclear framework.[130,131] It is thus a system where the addition of diffuse basis functions is essential if Gaussian-type orbitals are used. Slater-type orbitals, as opposed to Gaussian-type orbitals, exhibit the correct long-range behavior. The effects of adding diffuse functions to Slater-type basis sets should be insignificant in the applications studied here.

3. Results and Discussion

This discussion begins with some short notes on why there are problems with the LDA and standard GGA functionals in properly describing barrier heights (section 3A). The presentation of our results then follows, starting with an overview of the total set of reactions studied (section 3B). To be able to draw conclusions on the performance of density functionals for specific classes of reactions, we have then made separate analyses for four different cases: the hydrogen addition/unimolecular dissociation reactions (section 3C), the XH_2 systems (section 3D), the HOCO system (section 3E) and the H_3O system (section 3F). Following that, we present some conclusions about the general class of reactions involving hydrogen atoms (section 3G). We also investigate the importance of performing geometry optimizations (section 3H) and finally, the effects of using smaller basis sets are considered (section 3I). Tables with average errors (AEs) with standard deviations and mean absolute errors (MAEs) of barrier heights, MAEs of reaction energies, the errors in the energetics of the HOCO and H_3O systems, and the errors in atomization energies discussed in section 3E can be found in the Supporting Information. In the paper, energies are mostly given in eV, but in the Supporting Information the unit of energy is kcal mol^{-1}.

A. 'Normal' and 'Problematic' Systems. In the paper by Gritsenko et al.[132] a qualitative rule was proposed as to decipher how 'problematic' a molecular system is. The fraction n/m was shown to be a key concept, where m is the number of fragment orbitals (or centers) participating in a bond and n is the number of electrons in that bond. If n/m is noninteger the system is 'problematic' and if n/m is integer the system is 'normal'. Note that the concept of a 'bond' as used here, is generalized to extend over two *or more* atomic centers. As a matter of fact, the approximate LDA and GGA exchange are very different from exact (HF) exchange as they also mimic long-range/nondynamical correlation effects. Such an error, usually referred to as SIE-X (self-interaction error of DFT exchange), therefore turns out to be an advantage for 'normal' systems.[88−90] For a 'problematic' system, however, the long-range/nondynamical correlation effects are hampered and the LDA and standard GGAs will give a too negative E_{xc} leading to overstabilization of the particular molecular structure. This has been studied for the case of S_N2 reaction barriers ($n/m = 4/3$)[132] and A_2^+ systems (A = He, H_2O, NH_3; $n/m = 3/2$).[133] For these systems, an improvement of the exchange functional, which is the dominating contribution to the energy, will be more important than improving the correlation functional. The hydrogen abstraction and addition reactions considered in this paper, belong to the 'normal' systems, having three-center, three-electron bonds ($n/m = 3/3$) in their transition structures. In this case, improving the exchange functional will have less effect than improving the correlation functional. This has recently been demonstrated for the case of hydrogen abstraction reactions.[70,134] In the paper by Grüning et al.[70] it was noted that changing from the B88x to the OPTX exchange functional gave a dramatic improvement for 'problematic' systems (S_N2 barriers), while changing from a standard GGA (LYP) to an improved correlation functional like the meta-GGA LAP3 had a similar effect on the 'normal' systems (hydrogen abstraction barriers). The combination of OPTX and LAP3 (OLAP3) was shown to give the best overall results for barriers among a set of 17 density functionals (LDA, GGAs, and meta-GGAs). The improved performance of LAP3 is through the separate treatment of parallel and opposite spin correlation and its self-interaction free form. Functionals with the same features include the other meta-GGA correlation functionals studied here, i.e., B88c, B95, B98, VS98, KCIS, PKZB, and τ1. Some correlation functionals of the GGA type, such as the HCTH functionals, B97-1 and B97-2, are also similarly constructed but are not self-interaction free. Note that the n/m rule only tells us which part of the E_{xc} functional is most sensitive to changes. Both the exchange and correlation functionals will in most cases have an effect on the energetics.

B. Total Set of Reactions. In Figure 1 the average errors (AEs), with standard deviations, in the computed energies of the density functionals for the total set of 20 barriers are shown. The standard deviations are included to indicate the spread in the errors. As can be seen, the LDA and most of the GGA functionals systematically underestimate the barrier heights (Figure 1a). The magnitudes of the AEs are larger than 0.15 eV for most of the functionals. This disqualifies them for use in kinetics studies. It is only the HCTH functionals that exhibit AEs between −0.10 and −0.05 eV. The performance of these functionals is outstanding in this respect. Their improved functional form, and the fact that they have been fitted to large training sets, seems to have made them capable of reproducing these types of barriers. Note also the improvement in going from BLYP to OLYP with AEs of −0.22 and −0.15 eV, respectively. This seems to suggest that the OPTX exchange functional is better suited than the standard B88x functional to these systems, in agreement with a recent paper by Baker and Pulay[72] on a number of (mainly) organic reactions.

In Figure 1b the results for the meta-GGA functionals are shown. BLAP3, VS98 and Bmτ1 show similar performance to the HCTH functionals, but it is OLAP3 that is by far the most outstanding, with an AE of −0.02 eV. The AE is −0.09 eV for BLAP3, once again showing the improvement in going from B88x to OPTX. However, as discussed above, for these 'normal' systems it is the change of correlation functional that gives the largest improvement in energy. Thus going from BLYP to BLAP3, and from OLYP to OLAP3, raises the barriers by on average 0.13 eV, and reduces the mean absolute error (MAE) from 0.23 to 0.10 eV and from 0.17 to 0.07 eV, respectively. OLAP3 has the smallest MAE for the total set of barrier heights of all the functionals studied.

The results of the hybrid functionals, given in Figure 1c, show that all functionals, except B3LYP, have magnitudes of their AEs of less than 0.1 eV. The smallest MAE (0.07 eV) is found for B1B95-28 showing that a large amount of exact exchange is not necessarily needed for good descriptions of barrier heights. The MPW1K functional has a MAE of 0.10 eV, which might

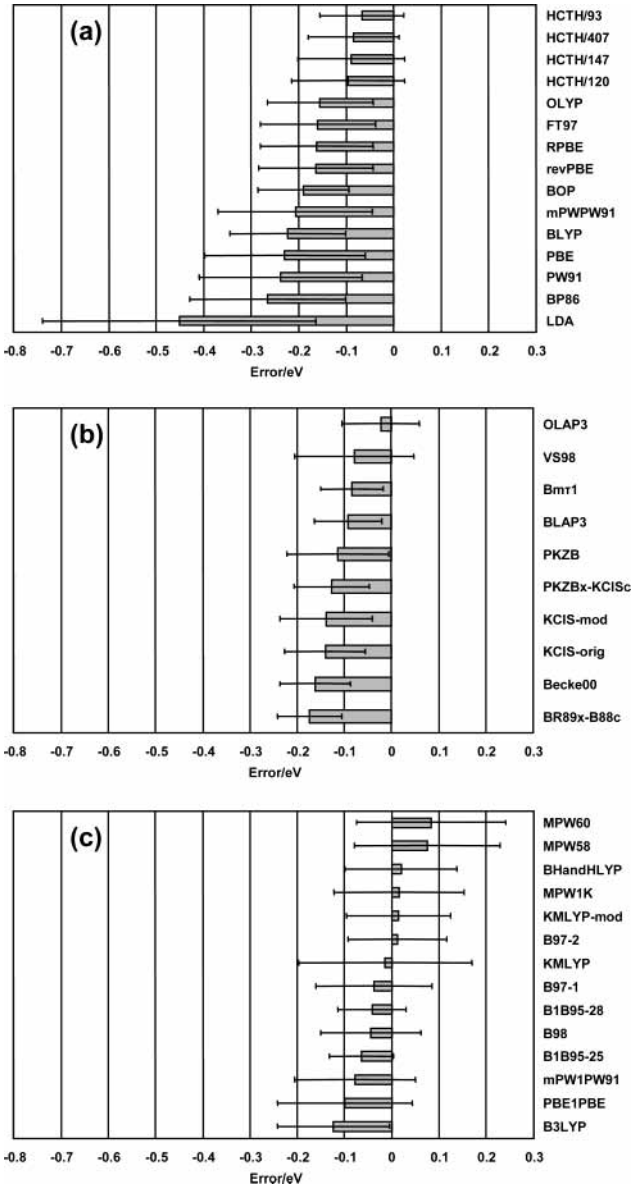

Figure 1. Average error with standard deviations (in eV) of the total set of barrier heights for (a) LDA and GGA, (b) meta-GGA, and (c) hybrid functionals.

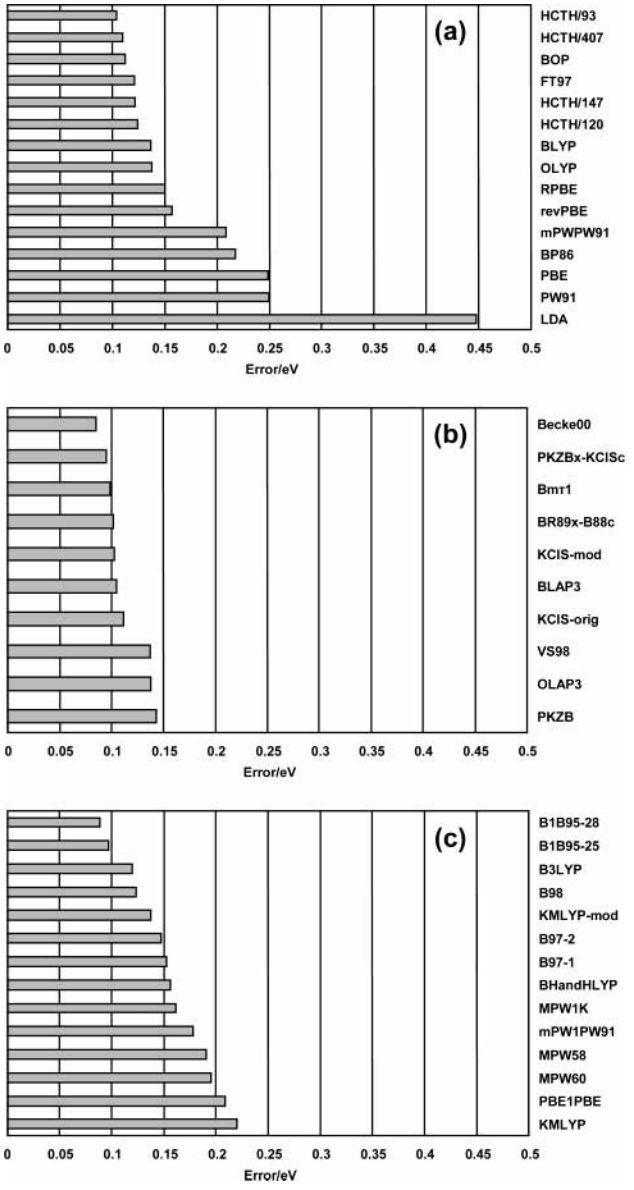

Figure 2. Mean absolute errors (in eV) of the total set of reaction energies for: (a) LDA and GGA, (b) meta-GGA, and (c) hybrid functionals.

be a bit disappointing considering it has been constructed with barrier heights in mind. However, it can be seen in Figure 1c that its *average* error for barrier heights actually is 0.015 eV whereas that for B1B95-28 is −0.04 eV. It seems that the predicted barrier heights of MPW1K all fall around the 'true' values with no systematic under- or overestimation, whereas B1B95-28 underestimates barrier heights more frequently. Thus, MPW1K should still be a reliable tool for predicting barrier heights. From the same figure it can be seen that its 'cousins', MPW58 and MPW60, which have larger amounts of exact exchange, in many cases overestimate barrier heights.

When it comes to reaction energies, the differences between the different classes of functionals are not that large. In Figure 2 the MAEs of reaction energies are shown. It can be seen that the meta-GGAs (Figure 2b) in general give the best reaction energies. All of these functionals have MAEs smaller than 0.15 eV and Becke00, PKZBx-KCISc, and Bmτ1 have MAEs smaller than 0.10 eV. Several of the GGAs (Figure 2a) also have MAEs between 0.10 and 0.15 eV, i.e., the HCTH functionals, BOP, FT97, BLYP, OLYP, and RPBE. The hybrid functionals (Figure 2c) are in general not better than the meta-GGAs when it comes to predicting reaction energies. B1B95-28, B1B95-25, B3LYP, B98, KMLYP-mod, and B97-2 give MAEs that are smaller than 0.15 eV, and the B1B95 functionals give MAEs smaller than 0.10 eV. The high-exact exchange functionals, with the exception of KMLYP-mod, do not perform that well for reaction energies and have MAEs of about 0.15−0.20 eV. The best overall performance is found for the meta-GGA Becke00, with a MAE of 0.08 eV.

C. Hydrogen Addition and Unimolecular Dissociation Reactions. The hydrogen addition reactions, i.e., the reactions of H+X to form HX where X is CO, HCHO, C_2H_2, or C_2H_4, and their reverse dissociation reactions are shown in Table 1. These reactions share very similar features: they have forward barriers of 0.1−0.2 eV, and are all quite exothermic with reaction energies of 0.8−1.8 eV. Figure 3 shows the AEs with standard deviations of hydrogen addition barriers and Figure 4 the same for the dissociation barriers.

For the case of hydrogen addition, the HCTH functionals outperform the other GGA functionals, with AEs of about −0.03

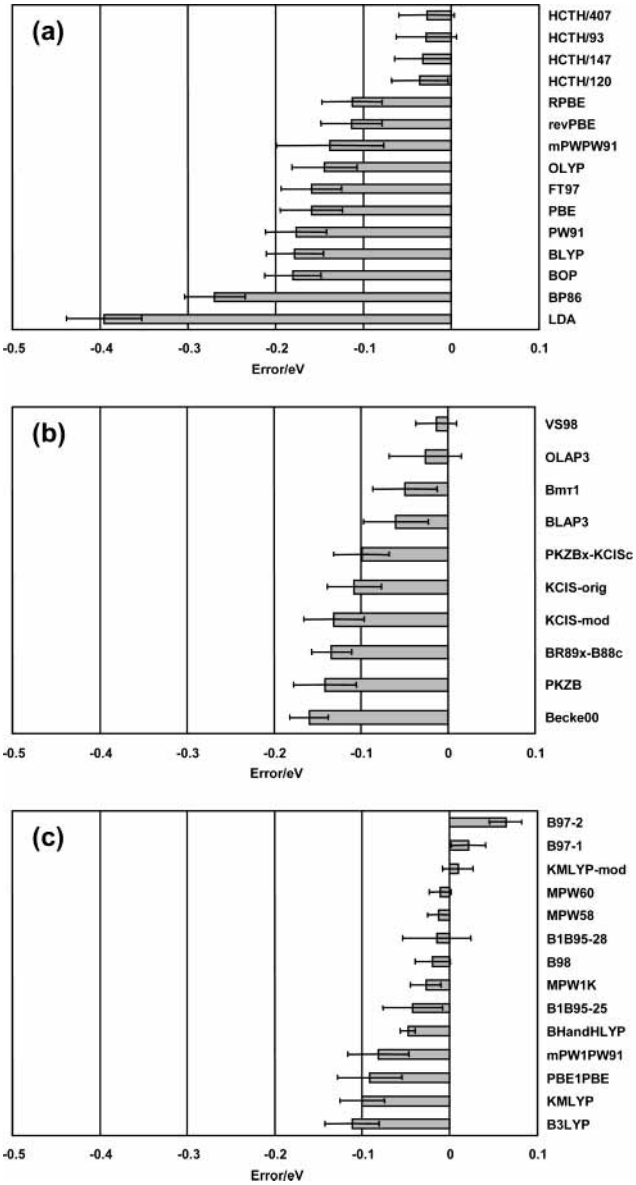

Figure 3. Average errors with standard deviations (in eV) of the barrier heights for hydrogen addition for (a) LDA and GGA, (b) meta-GGA, and (c) hybrid functionals.

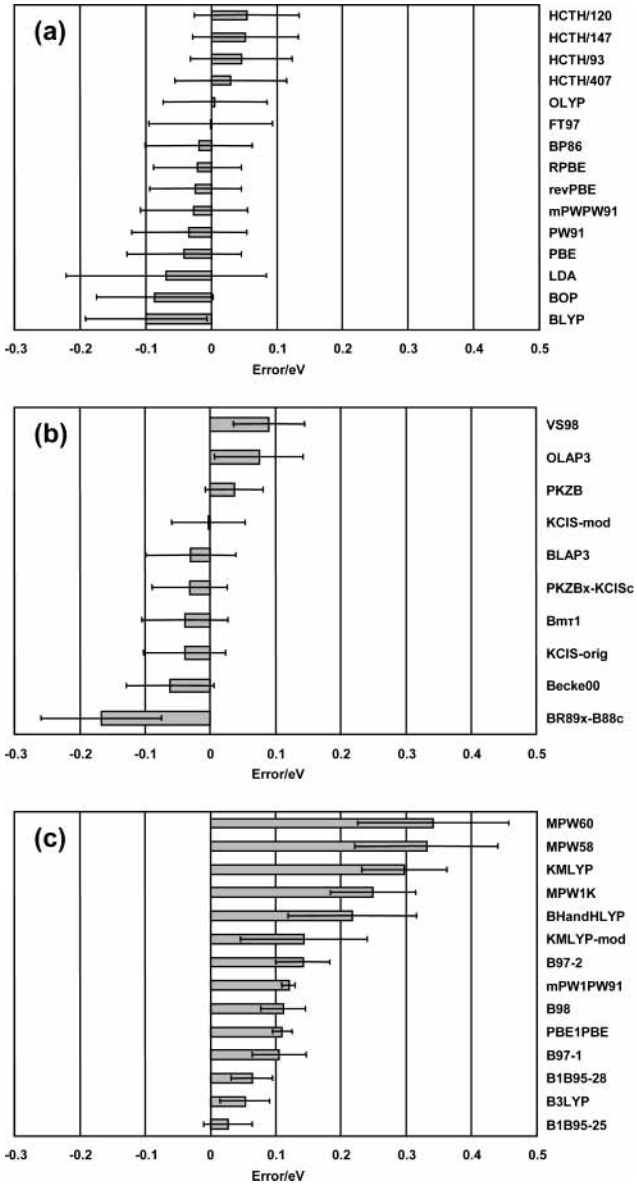

Figure 4. Average errors with standard deviations (in eV) of the barrier heights for unimolecular dissociation for (a) LDA and GGA, (b) meta-GGA, and (c) hybrid functionals.

eV (Figure 3a) and MAEs of 0.03−0.04 eV. Their main 'contenders', revPBE and RPBE, have AEs of −0.11 eV. VS98 stands out among the meta-GGA functionals with an AE of −0.01 eV (Figure 3b) and a MAE of 0.02 eV, but OLAP3 also performs well, with an AE of −0.03 eV and a MAE of 0.04 eV. Note that the majority of the GGAs and some of the meta-GGAs have average errors that are negative and of the same magnitude as the ab initio barriers. Thus, these functionals predict no or very low barriers for these reactions. Several of the hybrid functionals do very well for these reactions (Figure 3c): B98, B1B95-28, MPW58, MPW60, KMLYP-mod, and B97-1 all have AEs with magnitudes of 0.02 eV or smaller, and MPW58, MPW60, KMLYP-mod, and B97-1 also have MAEs of 0.02 eV or smaller. As can be seen from Figure 3, the standard deviations are all relatively small (smaller than or equal to 0.04 eV). This indicates that the errors in these barrier heights are all of a similar magnitude given a specific functional. One could therefore expect similar performance for the barrier heights of other reactions of the same type.

The reverse reactions of hydrogen addition, the unimolecular dissociation of the HX radicals, present a somewhat different story, as can also be seen in Figure 4. LDA and the GGAs all give AEs smaller than 0.1 eV, and all these functionals, except LDA, BLYP, and BOP, also give MAEs that are smaller than 0.1 eV. OLYP and FT97 have practically zero AEs, and OLYP, together with the HCTH functionals, also have the smallest MAEs (0.06 eV). The meta-GGAs, except BR89x-B88c, give results similar to the GGA functionals. KCIS-mod is the best-performing meta-GGA, with a zero average error and a MAE of 0.05 eV. PKZB also does quite well with an AE of 0.04 eV and a MAE of 0.04 eV. The B1B95 functionals and B3LYP give similar accuracy as the best GGAs and meta-GGAs, and B1B95-25 is the functional that gives the smallest overall MAE (0.03 eV). It is interesting to note that the MPWX functionals, together with BHandHLYP and KMLYP, give the worst results of all functionals, including LDA. The problem is that the hydrogenated species (HX) are overstabilized by the high-exact exchange functionals by about 0.2−0.4 eV, the only exception being KMLYP-mod, which gives an average overstabilization of 0.14 eV.

D. X+H_2 and XH+H Hydrogen Abstraction Reactions. The XH_2 systems have forward and backward reactions that

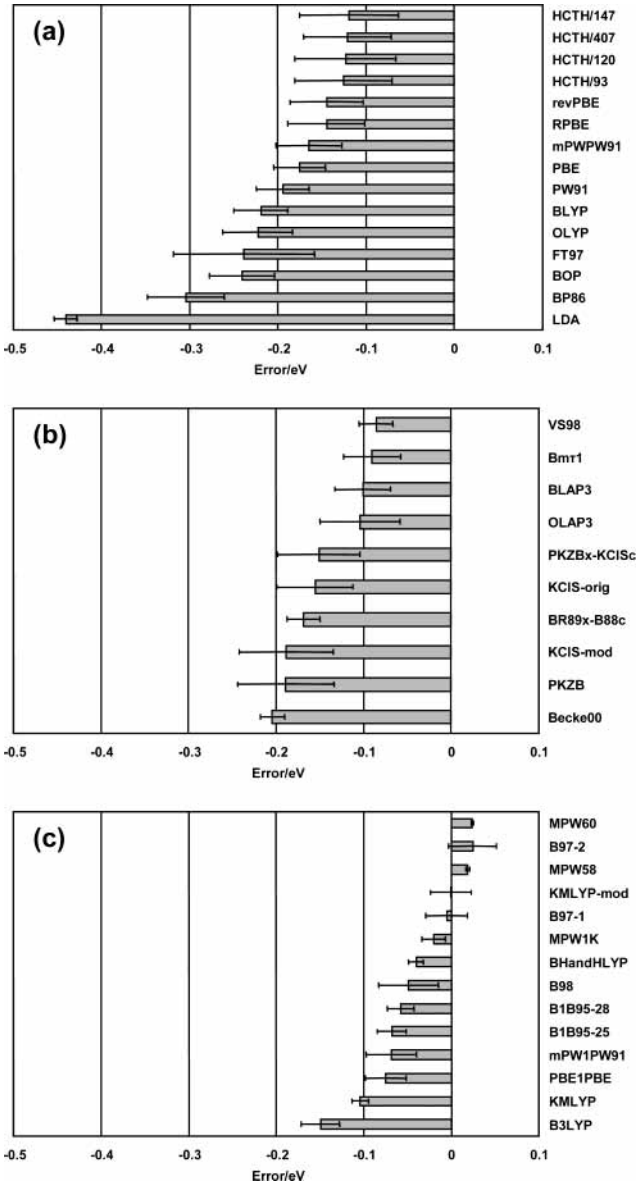

Figure 5. Average errors with standard deviations (in eV) of the barrier heights for XH+H reactions for (a) LDA and GGA, and (b) meta-GGA, and (c) hybrid functionals.

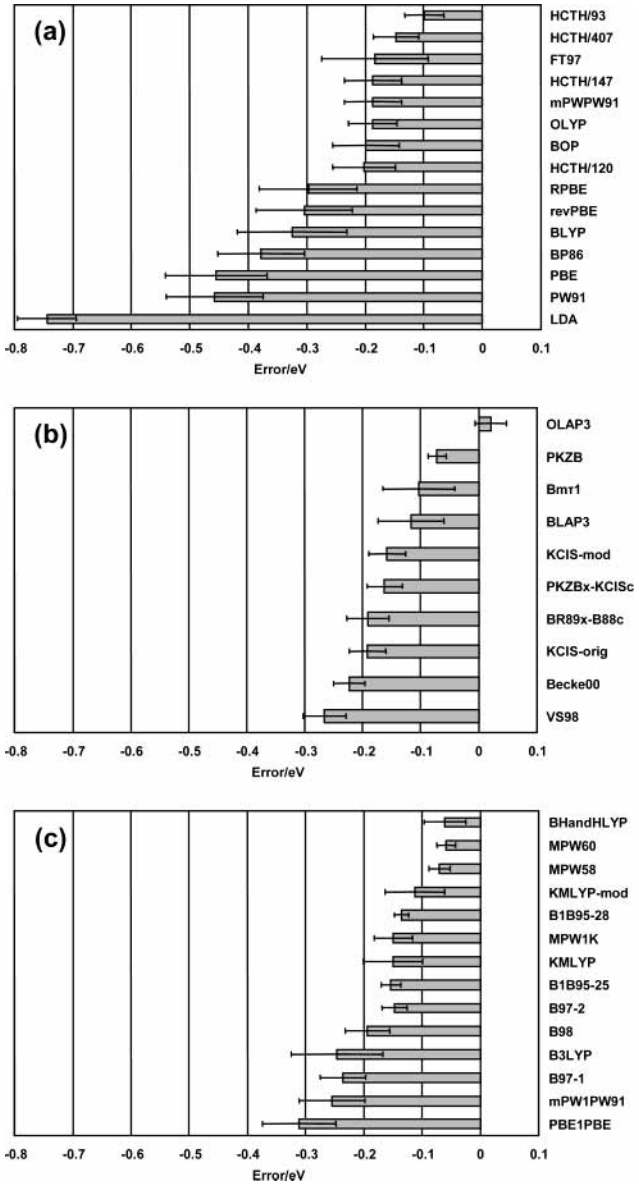

Figure 6. Average errors with standard deviations (in eV) of the barrier heights for $X+H_2$ reactions for (a) LDA and GGA, and (b) meta-GGA, and (c) hybrid functionals.

both can be classified as hydrogen abstraction reactions. The XH+H barriers are, as was shown in Table 1, about 0.1 eV for X = C, N and S, and 0.7 eV for X = CH_2. For $X+H_2$, the corresponding figures are 1.0−1.3 eV for X = C, N and S, and 0.3 eV for X = CH_2.

The AEs of XH+H and $X+H_2$ reactions are shown in Figures 5 and 6, respectively. Of the GGA functionals it is still the HCTH functionals that give the best results for the XH+H reactions, but the AEs are much more negative than for hydrogen addition (about −0.12 eV), whereas the difference in performance when compared to other GGAs is not that large. Since the AEs are larger in magnitude than the reference barrier heights for X = C, N, and S, and the barriers are all underestimated, this means that no barriers are found for these three reactions. The $X+H_2$ barriers seem to be difficult to describe. As can be seen from the average errors in Figure 6, these barriers are almost always underestimated. None of the GGAs have AEs smaller in magnitude than 0.1 eV for this case.

The meta-GGA functionals offer some improvement: VS98, Bmτ1, BLAP3, and OLAP3 all give higher barriers on average (AEs of around −0.1 eV) for XH+H than the HCTH functionals, but it is only OLAP3 and PKZB that perform clearly better than the GGAs for the $X+H_2$ reactions with AEs of 0.02 and −0.07 eV and MAEs of 0.03 and 0.07 eV, respectively. OLAP3 is the only functional that does not systematically underestimate the $X+H_2$ barriers.

The hybrid functionals perform very well for the XH+H reactions: it is only B3LYP and KMLYP that do not give AEs with magnitudes smaller than 0.1 eV. Four of them have MAEs of 0.02 eV or smaller, i.e., B97-1, MPW1K, MPW58, and KMLYP-mod. BHandHLYP together with MPW58 and MPW60 give the best performance of the hybrid functionals for $X+H_2$ barriers with AEs of about −0.06 eV and MAEs of 0.06−0.07 eV. When both forward and reverse barriers are included in the analysis it is MPW58 and MPW60 that show the most promising results. Since these functionals were optimized for the barrier height of a system of the XH_2 type, namely $CH_4+H \rightarrow CH_3+H_2$, this does make good sense. It also goes to show that the performance of the density functionals is very similar when comparing results for different XH_2 systems. Also, if the

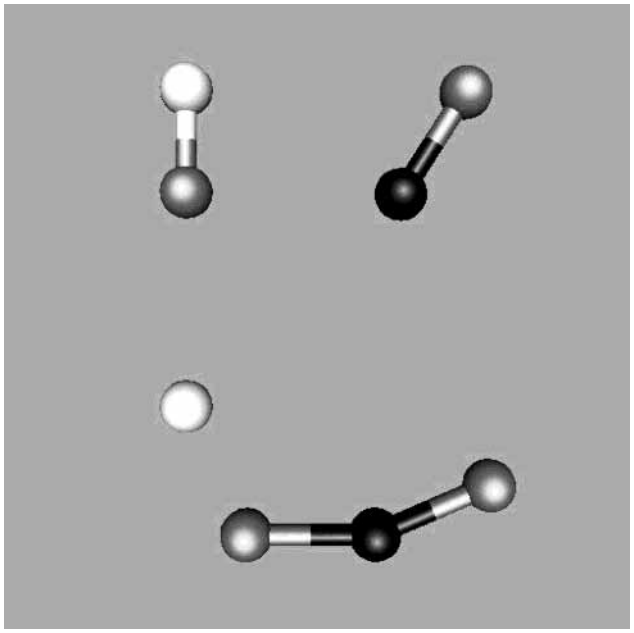

Figure 7. Geometries of *cis*-HOCO TS1 (top) and *cis*-HOCO TS2 (bottom). H atoms are white, carbon atoms black, and oxygen atoms gray.

reaction energy is included in the analysis it is seen that it is BHandHLYP that gives the best overall results for the XH_2 systems. These hydrogen abstraction reactions seem to be cases where hybrid functionals generally perform better than their nonhybrid counterparts, the only exception being OLAP3, which gives the best overall results for the $X+H_2$ barriers.

As in the case of the hydrogen addition barriers, the standard deviations are fairly small, both for the XH+H (0.00−0.08 eV) and $X+H_2$ barrier heights (0.01−0.09 eV).

One could therefore expect similar results also for other reactions of these types. Inspecting the performance for these two types of reactions, one sees quite different dependency of the performance of a functional on its functional form. For the XH+H barriers, the specific form of the DFT exchange is of minor importance, while changing the correlation functional and/or adding exact exchange can give quite significant differences in the performance. In the case of the $X+H_2$ barriers, also the proper choice of DFT exchange is very important. To illustrate these facts, note for instance the insignificant difference in AEs between BLYP and OLYP in Figure 5. However, when substituting the LYP correlation functional for LAP3, the XH+H barriers are raised by on average 0.12 eV. In Figure 6 one can see that the AE for the $X+H_2$ barriers is raised by 0.21 eV in going from BLYP to BLAP3, and further by 0.14 eV when going to OLAP3. Since the $X+H_2$ barriers are more sensitive to the change in exchange, one would expect that also mixing in exact exchange would lead to larger changes in energy for the $X+H_2$ barriers than for the XH+H barriers. This also seems to be the case. The average difference in BLYP and BHandHLYP XH+H barrier heights is 0.21 eV, and for the $X+H_2$ barriers the corresponding difference is 0.31 eV. The reasons for the differences in performance for these two types of reactions will need to be addressed in future work.

E. The HOCO System. The HOCO system is somewhat different from the other systems in this study as the forward and reverse reactions (OH+CO and $H+CO_2$) are not direct, but proceed through a collision complex (see ref 104 for details). As there are several saddle-point geometries we chose two of these as our forward and reverse barriers, respectively. These

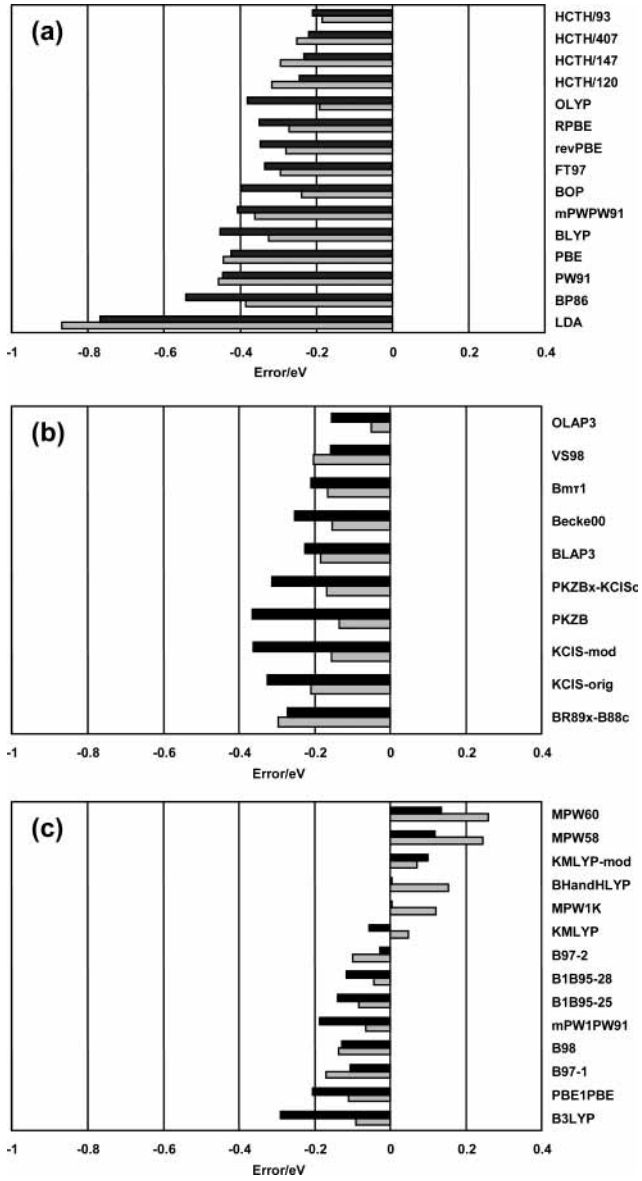

Figure 8. Errors in barrier height for *cis*-HOCO TS1 relative to OH+CO (black) and *cis*-HOCO TS2 relative to $H+CO_2$ (gray) for (a) LDA and GGA, (b) meta-GGA, and (c) hybrid functionals.

are shown in Figure 7. The first saddle point encountered in the OH+CO reaction is called *cis*-HOCO TS1 using the terminology of Yu et al.,[104] and for $H+CO_2$ it is called *cis*-HOCO TS2.

In Figures 8 and 9 we have summarized the errors of the energetics. There are three categories of errors in barrier heights. The first two are the errors in the forward (*cis*-HOCO TS1 vs OH+CO) and reverse (*cis*-HOCO TS2 vs $H+CO_2$) barriers, for which the reference energies are 0.11 and 1.1 eV, respectively (Table 1). The third one is the error in the barrier height of *cis*-HOCO TS2 relative to OH+CO. From a kinetic point of view, this latter energy difference is crucial as it is predicted to be a 'bottleneck' in the system, i.e., the lowest possible barrier the reaction has to proceed through, with a barrier height of 0.06 eV.[104] Thus this seems to be a crucial test of the density functionals.

The forward barrier, *cis*-HOCO TS1, is apparently rather difficult, since many functionals that have been performing well for the other reactions in this study have errors with a magnitude of 0.10−0.25 eV. There are a few functionals that give relatively small errors: OLAP3 (−0.04 eV), mPW1PW91 (−0.06 eV),

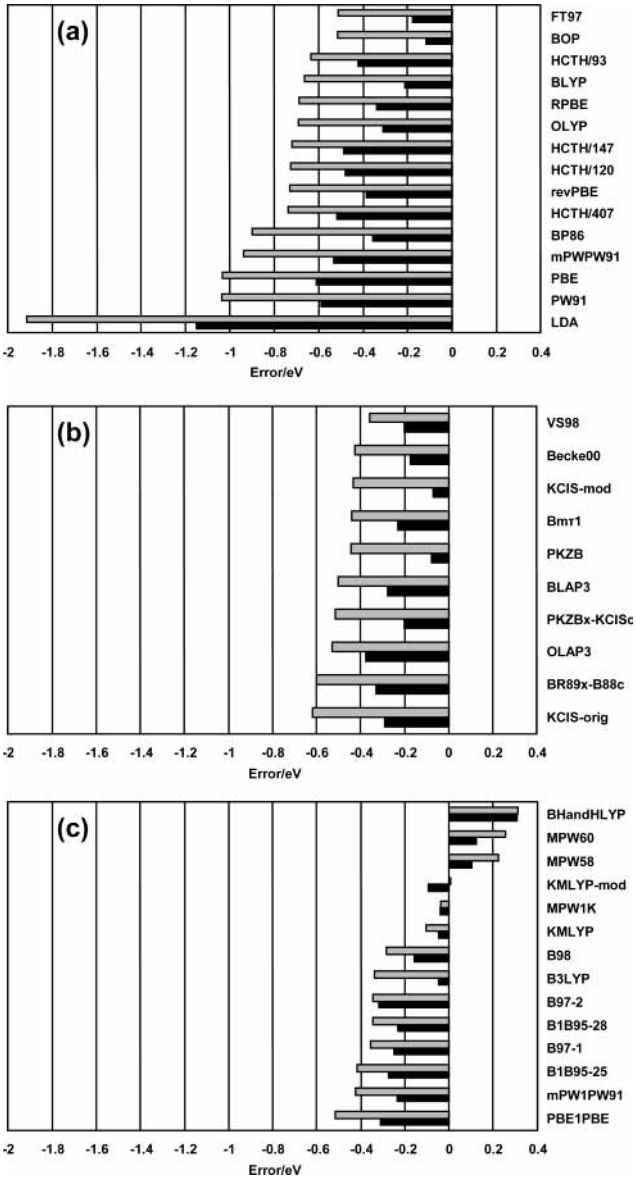

Figure 9. Errors in reaction energy, taken to be negative, for OH+CO reaction (gray) and errors in barrier height (in eV) of cis-HOCO TS2 relative to OH+CO (black) for (a) LDA and GGA, (b) meta-GGA, and (c) hybrid functionals.

B1B95-28 (−0.04 eV), and KMLYP (0.05 eV). All functionals except the ones with a large amount of exact exchange underestimate the barrier: LDA by 0.9 eV, the GGAs by 0.2 to 0.5 eV, the meta-GGAs by 0.04 to 0.3 eV, and the low-exact exchange hybrid functionals by 0.04 to 0.16 eV. The high-exact exchange hybrid functionals overestimate this barrier by 0.05 to 0.26 eV.

There are several reports in the literature, which clearly show the difficulties encountered by many density functionals in accurately describing barrier heights of reactions involving the OH radical.[47,50,52,57,58,60,70,72−80] The trends in performance seen for the OH+CO reaction seem to be a quite general feature for the class of reactions involving OH. From the work by Grüning et al.[70,135] it can be found that for a set of seven reactions involving OH, the AEs are the following: LDA −1.0 eV, GGAs −0.3 to −0.5 eV, and meta-GGAs −0.1 to −0.4 eV. The smallest AEs for the GGAs were found for HCTH/93 (−0.31 eV) and OLYP (−0.33 eV) and among the meta-GGAs, OLAP3 was clearly better than the rest with an AE of −0.13 eV, as compared to Bmτ1, BLAP3, Becke00, and PKZB that all had AEs of about −0.2 eV. From the results in the papers by Lynch et al.[52] and Kang and Musgrave,[57] some trends among hybrid functionals can be found. Low-exact exchange functionals, such as B3LYP and mPW1PW91, systematically underestimate OH reaction barrier heights by on average about −0.2 eV. This is not the case for high-exact exchange functionals. For instance, BHandHLYP overestimates most barriers and has an AE of 0.1 to 0.2 eV. Furthermore, MPW1K and KMLYP are both found to perform very well with AEs of about −0.02 eV and MAEs of about 0.04 eV. Barckholtz et al.[78] made transition-state theory calculations for the reactions of OH with C_6H_6 and found that B3LYP underestimated the barriers while MPW1K gave an overestimate, but in better agreement with experiment. In the work by Tokmakov and Lin[79] on the same reactions, it was also found that B3LYP gave a considerable underestimate of the barriers, while both KMLYP and MPW1K gave good results, the latter consistently giving the higher barriers. All of these observations comply very well with the performance of the density functionals for the OH+CO reactions, showing that there are clear trends common to many reactions involving OH. The reverse barrier, *cis*-HOCO TS2, is also difficult to reproduce and many functionals have errors of 0.10−0.25 eV. However, in this case there are three functionals that give errors smaller than 0.04 eV: BHandHLYP, B97-2, and MPW1K.

The reaction energy of this system seems to be extremely challenging, as can be seen in Figure 9. Note that the reaction energy has been defined to be *negative* in the figures for ease of comparison with the errors in the barrier height. Many of the functionals that have been showing good results for the other reactions now fail badly with errors of 0.2−0.5 eV. For instance, HCTH/407 overestimates the magnitude of the reaction energy by 0.5 eV. There are a few functionals that come within 0.1 eV of the reference energy (KCIS-mod, PKZB, B3LYP, MPW1K, MPW58, and KMLYP) but overall the results are not particularly good.

The main problem for predicting the reaction energy lies in the unbalanced description of atomization energies of CO_2 and CO. The OH radical seems to be fairly 'easy' to describe. All functionals except LDA, BP86, BLAP3, MPW58, MPW60, and KMLYP-mod give errors in the atomization energy of OH of less than 0.2 eV, and not less than 22 functionals give results within 0.1 eV of the experimental value. The atomization energies of CO_2 and CO are closely connected, and there are clear trends in the performance of density functionals for these two molecules. The problems encountered by density functionals for these two molecules show similar features to those encountered in the S_N2 reaction barriers, as briefly discussed in section 3A. The GGAs and the meta-GGAs with GGA exchange (BLAP3, Bmτ1 and OLAP3) all overstabilize (overbind) CO_2 by between 0.06 eV (FT97) and 1.15 eV (PBE). The errors of CO atomization energies are smaller, and some of these functionals actually underbind CO. Destabilization is mainly achieved by improving the exchange functional, as opposed to the barrier heights where the correlation functional was found to be more important. The errors in the atomization energies of CO_2 and CO for BLYP are 0.46 and 0.10 eV, respectively, and for OLYP 0.34 eV and −0.05 eV. Changing from the B88x to the OPTX functional thus destabilizes CO_2 by 0.12 eV and CO by 0.15 eV. Substituting the LYP correlation functional by the meta-GGA LAP3 functional, which gave a clear improvement for barrier heights, actually makes the results worse, with errors for OLAP3 of 0.69 eV for CO_2 and 0.14 eV for CO. The functionals with both meta-GGA exchange and correlation contributions show relatively small errors of between 0.25 eV

TABLE 2: Errors (in eV) of CO_2, CO, and OH Atomization Energies

functional	CO_2	CO	OH
KCIS-mod	−0.09	−0.21	0.05
PKZB	−0.06	−0.19	0.06
B3LYP	−0.08	−0.20	0.09
MPW1K	−0.85	−0.71	−0.17
MPW58	−1.43	−1.04	−0.27
KMLYP	−0.16	−0.30	0.11
KMLYP-mod	−1.48	−1.09	−0.47

(KCIS-orig) and −0.06 eV (PKZB) for CO_2 and −0.06 eV (KCIS-orig) and −0.21 eV (KCIS-mod) for CO. Including exact exchange also destabilizes both molecules. For instance, the high-exact exchange hybrid functional BHandHLYP underbinds both molecules and has errors in atomization energies of −1.48 eV for CO_2 and −0.97 eV for CO, which are considerable differences from the BLYP results. The trends discussed above are also clearly visible in the sequence of the GGAs, PBE, revPBE, and RPBE, and the low-exact exchange hybrid functional PBE1PBE, which all just differ in the exchange part. The errors in CO_2 atomization energies are (in the order above) 1.15 eV, 0.38, 0.26, and 0.07 eV, and in CO 0.39 eV, −0.02 eV, −0.07 eV, and −0.20 eV, respectively.

Good reaction energies can be more or less 'accidental' as seen in Table 2. Here the atomization energies obtained with the functionals that give a small error in reaction energies (less than 0.1 eV) are summarized. One can see that there are two different cases. First, KCIS-mod, PKZB, B3LYP, and KMLYP give relatively small errors in atomization energies with a fairly small underbinding of CO_2, a somewhat larger underbinding of CO, and an overbinding of OH that balances the other two errors. Second, for MPW1K, MPW58, and KMLYP-mod all three molecules have large underbinding errors and the errors of CO and OH again add up to cancel the CO_2 error. Thus there is a criterion of balance of atomization energy errors that has to be met, and of the functionals that give small errors in reaction energies not all give good atomization energies for all these three molecules.

Finally, we analyze the results for the 'bottleneck' barrier, the energy of *cis*-HOCO TS2 relative to the OH+CO asymptote. These are shown in Figure 9 alongside the errors in the reaction energy. It is seen that for all LDA, GGA, and meta-GGA functionals there are two effects that enhance the errors of this barrier. First of all, since on the reaction path the *cis*-HOCO TS2 is close to the free H+CO_2, it is only natural that the overestimation of the magnitude of the reaction energy for all these functionals also has an effect on this saddle point. Second, functionals that do give good results for the reaction energy can still underestimate barriers where a hydrogen atom is involved. This casts some serious doubt on the usefulness of these functionals for the HOCO system. Functionals that have been promising for other reactions give abysmal results for this barrier. The HCTH functionals underestimate the barrier by 0.6−0.7 eV, and the OLAP3 result is also 0.5 eV below the reference energy. Of the GGA and meta-GGA functionals, VS98 is the best, with an error of 'only' 0.35 eV. As most hybrid functionals have many less problems with hydrogen atom reactions, the main problem for these functionals, except for B3LYP, is the reaction energy. Three high-exact exchange functionals, BHandHLYP, MPW58, and MPW60, underestimate the magnitude of the reaction energy, as opposed to all other functionals, and thus also overestimate this barrier by 0.2−0.3 eV. There are two functionals that give errors in the barriers that are not too large. KMLYP-mod and MPW1K have errors of 0.01 and −0.03 eV, respectively.

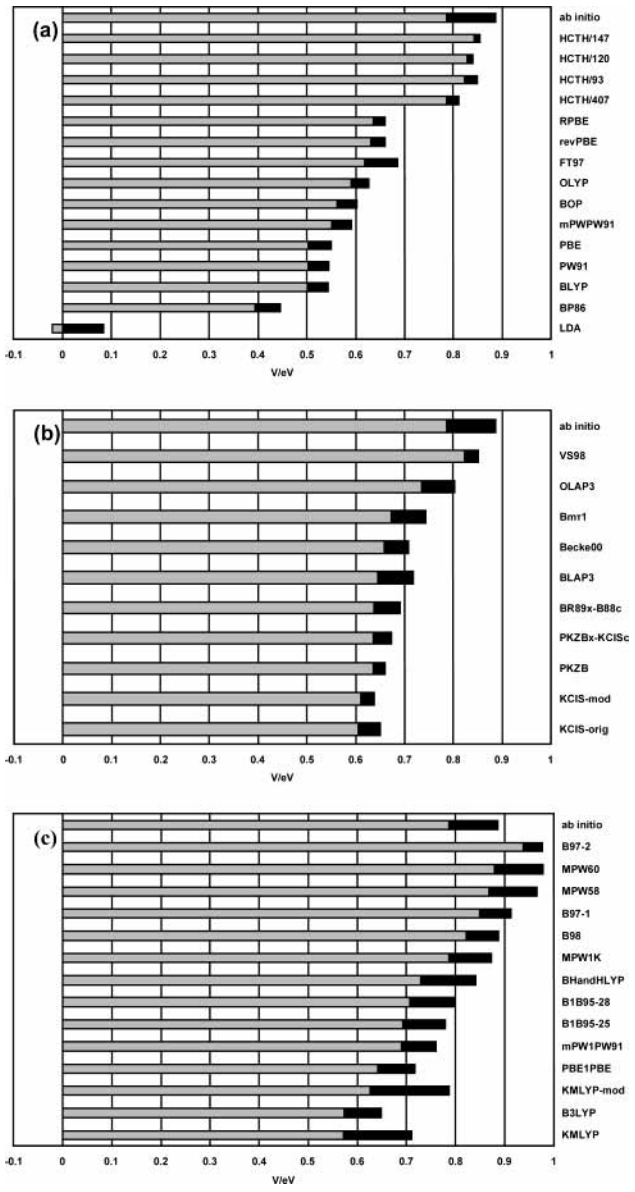

Figure 10. Reaction energy (gray) and barrier height (black) (in eV) of the H+H2O reaction compared to the ab initio reference energies for (a) LDA and GGA, and (b) meta-GGA, and (c) hybrid functionals.

In conclusion, the HOCO system constitutes a great challenge to DFT. It is only MPW1K, KMLYP, and KMLYP-mod that show a qualitatively, or semiquantitatively, correct description of the energetics of the system. All other functionals fail badly for at least two of the four relative energies we have been analyzing. KMLYP gives the overall best description of this system as it also gives rather small errors in the atomization energies. It would be interesting to investigate the performance (while also optimizing the geometries) of MPW1K, KMLYP, and KMLYP-mod for the numerous minima and saddle points on the potential surface of the HOCO system.

F. H_3O. The final system we consider in this paper is that of the addition of a hydrogen atom to H_2O to form the (metastable) H_3O species which has a forward barrier of 0.9 eV and a reaction energy of 0.8 eV (Table 1). In Figure 10 the actual reaction energies and barrier heights obtained with all the functionals are compared with the reference ab initio values. The LDA predicts H_3O to be a minimum on the potential energy surface and it gives an energy difference between H_3O and the saddle point (the reverse barrier) that is almost exactly equal to the ab

initio value. Applying a gradient correction obviously helps in destabilizing H_3O, but the forward barrier is still underestimated by at least 0.2 eV with all GGA functionals except the HCTH functionals, which underestimate the barrier by 0.03−0.07 eV. All GGA functionals predict reverse barriers that are clearly too small. The meta-GGA functionals do not in general perform differently from the 'better half' of the GGA functionals. VS98 and OLAP3 have errors within 0.1 eV for the forward reaction. It is among the hybrid functionals that we find the best performance for this system. MPW1K does extremely well and has a maximum error of only 0.01 eV. Several of the other functionals (B1B95-28, BHandHLYP, B98, B97-1, MPW58, MPW60, and B97-2) have errors of the forward barrier within 0.1 eV. It seems that the problem with the reverse barrier can be solved using hybrid functionals. No less than six functionals (BHandHLYP, B1B95-25, B1B95-28, MPW1K, MPW58, and MPW60) have errors within 0.015 eV.

G. Hydrogen Atom Reactions. It has been seen that for the hydrogen addition, XH+H, H+H_2O, and H+CO_2 (in the HOCO system) reactions, the density functionals basically follow the same trends in describing the barrier heights. It will therefore be very instructive to determine which functional gives the most accurate barrier heights for the general class of reactions where a hydrogen atom is one of the reactants. In Figure 11 we show the average errors of this type of reaction. Seven of the hybrid functionals have magnitudes of AEs of 1 kcal mol^{-1} (0.04 eV) or smaller: MPW1K, B97-1, MPW58, KMLYP-mod, MPW60, BHandHLYP, and B98. These functionals also give MAEs of 1 kcal mol^{-1} or smaller. These should therefore be the recommended functionals to use for hydrogen atom reaction barriers based on the results presented here. If a GGA is preferred, the HCTH functionals are by far the best choice with AEs of −0.09 eV. Of the meta-GGAs, VS98 and OLAP3 are recommended since they have AEs of −0.06 and −0.08 eV, respectively.

H. Geometry Optimization. There is of course a risk that a seemingly good functional might be consistent with ab initio results at given geometries, but that the agreement only is fortuitous and that the coordinate dependence of the functional does not resemble the ab initio potential surface at all. Of course, a good functional should be just as good at predicting saddle-point geometries as the best ab initio methods. The deviation from the 'true' geometry *is* of course a crucial test of any functional and has also to be made to give a complete description of its performance. This test was made for the H+CO reaction.

Results for nine different density functionals for the H+CO energies are summarized in Table 3, both for the fixed ab initio reference geometry and the actual barrier height, where both the CO bond length and the H−CO saddle point geometry have been optimized. Also shown are the optimized geometries and the ab initio reference values. The nine functionals fall into three main categories: (A) GGAs and meta-GGAs (HCTH/407, VS98, OLAP3), (B) low-exact exchange hybrid functionals (B97-1, B97-2, B1B95-25), and (C) high-exact exchange hybrid functionals (MPW1K, BHandHLYP, KMLYP-mod). The functionals in category A show a dramatic change (50−100%) in barrier height in going from fixed to optimized geometry, whereas B and C show more moderate changes of about 20% and 1−10%, respectively. The size of the change in barrier height correlates with the size of the change in the C−H distance at the saddle point geometry. For the GGAs and meta-GGAs, the C−H distance is 0.2−0.3 Å larger than in the ab initio geometry; for the hybrid functionals in category B, the difference is 0.15−0.2 Å and for C it is only 0.02−0.12 Å. It is also seen

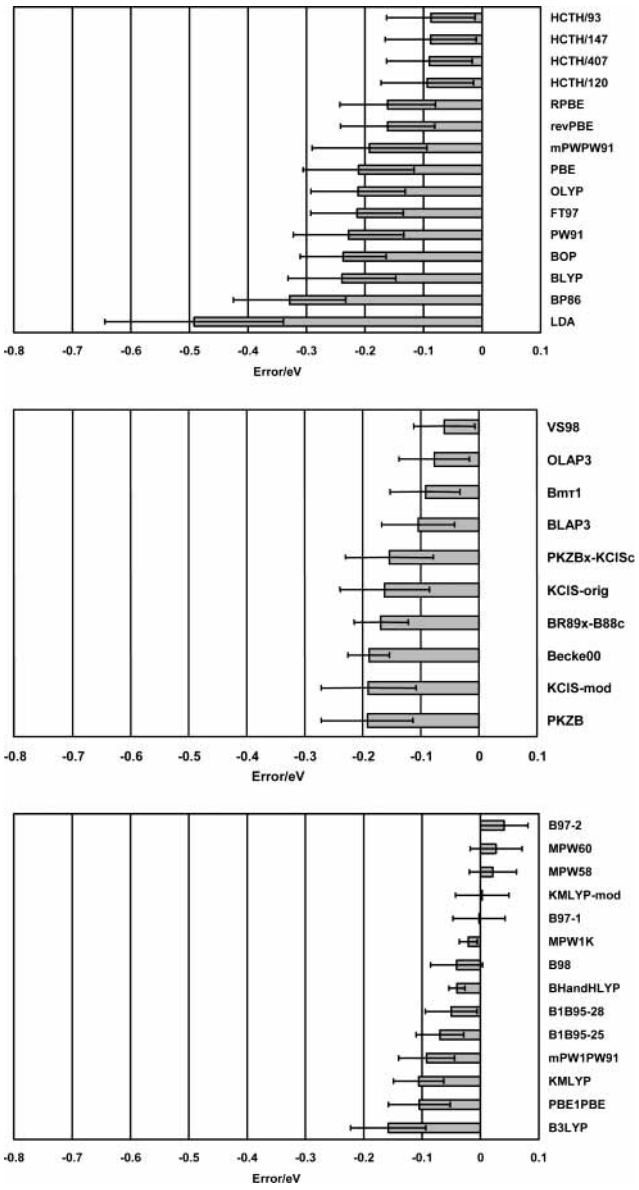

Figure 11. Average errors with standard deviations (in eV) of the barrier heights for H atom reactions for (a) LDA and GGA, (b) meta-GGA, and (c) hybrid functionals.

that functionals with a large amount of exact exchange underestimate the CO distance in H−CO by about 0.02 Å. This has little effect on the barrier heights in going from fixed to optimized geometry since the bond length of CO also is underestimated by about the same amount.

Since there is a dramatic increase in the HCTH/407, VS98, and OLAP3 barrier heights upon geometry optimization, it could thus well be that the AE in hydrogen addition barrier heights would become more positive if one optimizes the geometries. For all functionals, the barrier heights do increase upon optimizing the geometry. This has the effect that for most functionals the error in barrier height becomes smaller. In contrast, for VS98 there is basically no change in magnitude of the error, the barrier only goes from being lower to being higher than the reference barrier. Also, since the B97-2 barrier was already too high by 0.05 eV, the error increases to 0.09 eV in this case. It can be concluded that the hybrid functionals give better agreement with the ab initio saddle-point geometry, at least for the critical C−H distance. The nonhybrid functionals, HCTH/407, OLAP3, and VS98, give quite accurate equilibrium

TABLE 3: Barrier Heights (in eV) of Fixed (ab initio) and Optimized Geometries for H+CO and Optimized Geometries for Density Functionals and the Reference MRCI+Q Values

	barrier height		CO[a]	H−CO saddle point[a]		
functional	fixed geometry	opt. geometry	R_e	R_{CH}	R_{CO}	HCO angle
HCTH/407[b]	0.079	0.145	1.129	2.15	1.132	116.7
VS98[b]	0.109	0.155	1.131	2.07	1.134	116.7
OLAP3[b]	0.059	0.116	1.132	2.12	1.135	118.8
B97-1[c]	0.142	0.169	1.128	2.02	1.132	116.2
B97-2[c]	0.185	0.217	1.125	2.03	1.129	116.3
B1B95-25[c]	0.079	0.100	1.124	2.04	1.127	116.2
BHandHLYP[c]	0.082	0.090	1.113	1.97	1.117	116.9
MPW1K[c]	0.093	0.104	1.116	2.00	1.119	116.0
KMLYP-mod[c]	0.136	0.137	1.107	1.88	1.117	116.7
MRCI+Q (ref 94)	0.156	0.156	1.132	1.861	1.137	117.3
FCC/CBS//MRCI+Q	0.132	0.132	1.132	1.861	1.137	117.3

[a] CO and H−CO bond distances in angstroms and angles in degrees. [b] The ADF calculations were made using an even-tempered quadruple zeta basis set (ET-QZ3P). [c] With Gaussian 03 the geometries were optimized using the aug-cc-pVTZ basis set and energies calculated with aug-cc-pVQZ.

geometries, but there are larger discrepancies in the saddle-point geometry. The fact that the barrier heights, though not the saddle point geometries, obtained with the functionals tested agree very well with the reference energy, does not guarantee that these functionals are the most suitable for kinetics and dynamics studies. The potential surface should also be accurate in directions perpendicular to the reaction coordinate, and an accurate width of the barrier is crucial for quantum dynamics.

I. Basis Set Effects. To run calculations on larger systems, like for instance water clusters, the use of quadruple-ζ (QZ) basis sets is generally not computationally feasible.

To check the effects of using smaller basis sets, calculations were run with double-ζ (DZ) and triple-ζ (TZ) basis sets, as described in section 2. With one exception, the differences in energetics between the basis sets are relatively small. For the H_3O system, a change in basis set can, however, lead to dramatically different results, as mentioned in section 2. In going from a double-ζ to a triple-ζ STO basis set in ADF the reaction energy drops by 0.3−0.4 eV. The differences between triple-ζ and quadruple-ζ basis set results are only about 0.05−0.10 eV. With Gaussian 03, the change in going from a double-ζ to a triple-ζ GTO basis set is only 0.06−0.07 eV, but going to the quadruple-ζ basis set lowers the reaction energy by between 0.02 (mPWPW91) and 0.9 eV (MPW60). Among the hybrid functionals the smallest difference is 0.16 eV (B3LYP).

Next, we discuss H atom barriers and reaction energies. Since H_3O constitutes a rather special system, which is not representative of most chemical reactions, energetics discussed here are with the results for the H_3O system excluded. In going from the DZ to the TZ basis set using ADF, the AE in H atom barrier heights is lowered by 0.01−0.02 eV, and between the TZ and QZ basis sets the differences are practically zero. With Gaussian 03, the average H atom barrier height increases by 0.02−0.04 eV in going from the DZ to the TZ basis set, and by up to 0.03 eV going from TZ to QZ. The differences in the MAE of reaction energies are also relatively small. The difference between DZ and TZ results with ADF is 0.00−0.03 eV, and between TZ and QZ it is 0.00−0.02 eV. With Gaussian 03 the maximum change in MAE is 0.07 eV going from DZ to TZ, and 0.04 eV going from TZ to QZ.

The relatively small differences between the basis sets show that there is a possibility to also obtain results of comparable accuracy to the results using QZ basis sets also for much larger systems than have been considered in this paper. The average errors discussed in this section can be found in the Supporting Information.

4. Conclusions

In this study we have shown the performance of a number of density functionals, some 'standard' and some novel, for the prediction of classical barrier heights and reaction energies for reactions involving hydrogen. Some conclusions can be drawn on the performance of the different classes of approximate density functionals for the total set of reactions:

(i) Hybrid functionals with a large percentage (40−60%) of exact exchange, i.e., BHandHLYP, MPW1K, MPW58, MPW60, and KMLYP-mod, perform well for barrier heights, but less well for atomization and reaction energies.

(ii) Some hybrid functionals with a more modest amount (20−30%) of exact exchange and with an improved form of the correlation functional, i.e., B1B95-28, B97-1, B97-2, and B98, do just as well for most barrier heights as the functionals mentioned above, an important exception being the HOCO system, but in addition also give better atomization and reaction energies.

(iii) Meta-GGA functionals, which do not contain exact exchange but depend on the kinetic energy density and/or the Laplacian of the density, can perform almost as well as the hybrids for predicting barrier heights. In this context VS98 and especially OLAP3 have shown great promise. The latter also shows that the LAP3 correlation functional is an improvement over the LYP functional for the barriers of these 'normal' systems, since BLAP3 and OLAP3 give significantly improved results compared to BLYP and OLYP. There is also a small but clear improvement in using the OPTX exchange functional instead of the 'standard' B88 functional, since OLAP3 performs better than BLAP3. The meta-GGAs in general also give quite accurate reaction energies and Becke00 is the functional that gives the smallest overall mean absolute error for reaction energies.

(iv) Pure GGA functionals can also provide results that are comparable to the best meta-GGA results and only somewhat worse than the best hybrid results. This is demonstrated by the HCTH functionals that outperform all the other GGAs for the prediction of barrier heights and also do quite well for reaction energies. Differences between the four versions tested here are small. It seems, however, that HCTH/93 and HCTH/407 are somewhat better for barrier heights. Since GGAs are considerably less computationally demanding than hybrids for large systems, the HCTH functionals can provide a good alternative whenever computational efficiency is a major issue. The water dimer is included in the training sets for HCTH/120, HCTH/147, and HCTH/407 and one would therefore assume that these

functionals should give a good description of liquid water and water ice. It was indeed shown in the paper by Tuma et al.[136] that several hydrogen-bonded complexes were well described with HCTH/120 and in another paper by Boese et al.[117] it was shown that liquid water was well described using HCTH/120 in a Car−Parinello simulation. This, together with their improved treatment of barrier heights, would suggest that these functionals are suitable for simulating chemical reactions on ice surfaces.

One can also see clear trends in the performance of density functionals for specific classes of reactions:

(v) The four hydrogen addition reactions studied all involve a relatively low forward barrier (0.1−0.2 eV). The functionals that seem best suited for this kind of process are the meta-GGA VS98 and the hybrid functionals B97-1, MPW58, MPW60, and KMLYP-mod. The reverse dissociation reaction seems more difficult, and here the GGAs OLYP and HCTH/N, the meta-GGAs KCIS-mod and PKZB, and the hybrid functionals B1B95-25, B1B95-28, and B3LYP are doing quite well. The best description of both forward and reverse processes is given by the HCTH functionals, B1B95-25, and B1B95-28.

(vi) The $X+H_2$ reaction barriers are almost always underestimated and errors tend to be relatively large. The meta-GGA OLAP3 does very well, however (AE: 0.02 eV, MAE: 0.03 eV). The high-exact exchange hybrid functionals BHandHLYP, MPW58, and MPW60 also give good $X+H_2$ barriers, but they are systematically underestimated by on average 0.06−0.07 eV. The latter two functionals also do very well for the reverse XH+H reaction barriers. This is not surprising as they were optimized for a system of this type ($CH_4+H \rightarrow CH_3+H_2$). The XH+H barriers are also well described by B97-1 and KMLYP-mod. Including reaction energies, it is BHandHLYP that gives the best overall description of the XH_2 systems. In this case, OLAP3 is the best performing nonhybrid functional.

(vii) As for the reactions studied in this work that are most relevant to surface astrochemistry, the barriers to the hydrogen addition, and XH+H reactions, the hybrid functionals B97-1, MPW58, MPW60, and KMLYP-mod give the best results with AEs of 0.00−0.01 eV and MAEs of 0.02 eV. The best nonhybrid functional is the meta-GGA VS98 with an AE of −0.05 eV and a MAE of 0.05 eV.

(viii) The HOCO system poses a great challenge to DFT. It seems that only a few high-exact exchange hybrid functionals (MPW1K, KMLYP, and KMLYP-mod) are able to give a reasonable description of the potential energy surface. Most functionals have problems due to the unbalanced description of atomization energies of CO and CO_2 and/or systematic difficulties in describing potential barriers for reactions involving the OH radical and reactions of the hydrogen atom. Only KMLYP provides an overall good description of barrier heights, reaction energies *and* atomization energies. Note that functionals that do not contain a large amount of exact exchange fail rather badly for this reaction. It is suggested that this system should be considered as a prototype of complex-forming reactions. Anyone interested in constructing density functionals for these types of processes should have HOCO as an ultimate test.

(ix) The formation of the metastable H_3O species from $H+H_2O$ is also a challenge for density functionals. Standard GGA functionals underestimate the reaction energy (and barrier) by up to 50%. The performance is consistent with the problems of describing hydrogen addition barriers. However, most of the functionals that do well for the barrier heights in this study give good results for this system as well.

(x) For the general class of reaction barriers where a hydrogen atom is one of the reactants, the MPW1K, B97-1, MPW58, KMLYP-mod, MPW60, BHandHLYP, and B98 hybrid functionals were shown to provide the best performance with magnitudes of the average errors and mean absolute errors of barrier heights of 1 kcal mol^{-1} (0.04 eV) or smaller.

(xi) The use of double-ζ and triple-ζ basis sets seems to give results that are of comparable accuracy to the results obtained with the larger quadruple-ζ basis sets. Therefore, one should also be able to study much larger molecular systems and expect similar accuracy as for the small systems that have been considered in this work.

Finally, based on this study our recommendations for functionals to be used for studying chemical reactions similar to ours, are the following:

(xii) The functional that is most reliable in giving good barrier heights is MPW1K, as it is able to give a correct overall description of relative energies of all the systems in this study, including the difficult HOCO system. Its greatest shortcoming is the description of the unimolecular dissociation reactions where it overestimates the barriers by 0.2 eV. As was pointed out by Boese et al.[128] it is not well suited for the study of the energetics and geometries of stable molecules.

(xiii) If a balanced description of barrier heights and reaction energies is sought, the B1B95-28 hybrid functional seems to be the best alternative. It gives the second smallest mean absolute error both for reaction energies (after Becke00) and the total set of barrier heights (after OLAP3) of all the functionals. It is therefore recommended to use the original form of B1B95 with 28% exact exchange instead of the one implemented in Gaussian 03, which has 25%.

There are some issues that have not been covered in this work, but are of great importance to kinetics and dynamics studies. To cover entropic effects properly, a good description of the curvature of the potential in directions perpendicular to the reaction path is also needed. If a quantum mechanical treatment of nuclear motion is used, not only the height, but also the width of the potential barrier is important to properly describe tunneling. See ref 59 for a discussion on this in connection with the $H+H_2$ reaction. As stated, geometry optimization also has to be considered to give a complete picture of the quality of the density functionals. These issues need to be addressed in later work. The use of different basis sets and in some cases non-self-consistent calculations introduces small uncertainties in the comparison of results. To establish a completely consistent picture, all calculations would have to be performed on an equal footing. This is also something that needs more attention in future work.

It has been shown that for 10 reactions involving hydrogen there are density functionals that give results comparable to high-level ab initio methods. However, the performance of the methods can vary considerably from system to system and still the use of DFT for kinetics will involve testing the methods on model systems that will give a hint as to whether they are reliable for this type of system or not.

We do believe that calculations of these reactions on ice surfaces should be not only computationally feasible, but also sufficiently accurate for our purposes. It is our hope that this study will be helpful for those wanting to study systems similar to the ones in this paper.

Acknowledgment. Prof. G. J. Kroes at Leiden Institute of Chemistry, and Prof. E. F. van Dishoeck and Dr. H. J. Fraser at Leiden Observatory, are gratefully acknowledged for useful

discussions and for comments on this manuscript. We would also like to thank Dr. S. J. A. van Gisbergen at Vrije Universiteit, Amsterdam, for many helpful discussions on DFT calculations. S.A. is grateful for funding from the Spinoza prize awarded to Prof. van Dishoeck from The Netherlands Organization for Scientific Research (NWO).

Supporting Information Available: Energetics and geometries of reference data. Average errors, standard deviations, and mean absolute errors of barrier heights. Mean absolute errors of reaction energies. Errors in HOCO and H_3O energetics. Atomization energies of OH, CO, and CO_2. Basis set dependence of results for barrier heights and reaction energies. All energies are given in kcal mol^{-1}. The material is available free of charge via the Internet at http://pubs.acs.org.

References and Notes

(1) van Dishoeck; E. F.; Hogerheijde, M. R. In *Origin of Stars and Planetary Systems*; Lada, C. J., Kylafis, N., Eds.; Kluwer: Dordrecht, 1999; p 97.
(2) Ehrenfreund, P.; Fraser, H. J. In *Solid State Astrochemistry*; Pirronello, V., Krelowski, J., Eds.; Kluwer: Dordrecht, 2003; p 317.
(3) Boogert, A. C. A.; Ehrenfreund, P. In *Astrophysics of Dust*; Witt, A. N., Clayton, G. C., Draine, B. T., Eds., 2004; in press.
(4) Woon, D. E. *Astrophys. J.* **2002**, *569*, 541.
(5) Watanabe, N.; Kouchi, A. *Astrophys. J.* **2002**, *571*, L173.
(6) Watanabe, N.; Shiraki, T.; Kouchi, A. *Astrophys. J.* **2003**, *588*, L121.
(7) Hiraoka, K.; Sato, T. *Radiat. Phys. Chem.* **2001**, *60*, 389.
(8) Hiraoka, K.; Sato, T.; Sato, S.; Sogoshi, N.; Yokoyama, T.; Takashima, H.; Kitagawa, S. *Astrophys. J.* **2002**, *577*, 265.
(9) Kohn, W.; Sham, L. J. *Phys. Rev.* **1965**, *140*, A1133.
(10) Parr, R. G.; Yang, W. *Density Functional Theory of Atoms and Molecules*; Oxford: New York, 1989.
(11) Koch, W.; Holthausen, M. C. *A Chemist's Guide to Density Functional Theory*; Wiley: Weinheim, 2000.
(12) Dirac, P. A. M. *Proc. Camb. Philos.* **1930**, *26*, 376.
(13) Slater, J. C. *Phys. Rev.* **1951**, *81*, 385.
(14) Vosko, S. H.; Wilk, L.; Nusair, M. *Can. J. Phys.* **1980**, *58*, 1200.
(15) Becke, A. D. *Phys. Rev. A* **1988**, *38*, 3098.
(16) Perdew, J. P. *Phys. Rev. B* **1986**, *33*, 8822 (Erratum: *Phys. Rev. B* **1986**, *34*, 7406).
(17) Lee, C.; Yang, W.; Parr, R. G. *Phys. Rev. B* **1988**, *37*, 785.
(18) Perdew, J. P.; Chevary, J. A.; Vosko, S. H.; Jackson, K. B.; Pederson, M. R.; Singh, D. J.; Fiolhais, C. *Phys. Rev. B* **1992**, *46*, 6671 (Erratum: *Phys. Rev. B* **1994**, *48*, 4978).
(19) Perdew, J. P.; Burke, K.; Wang, Y. *Phys. Rev. B* **1996**, *54*, 16533 (Erratum: *Phys. Rev. B* **1998**, *57*, 14999).
(20) Perdew, J. P.; Burke, K.; Ernzerhof, M. *Phys. Rev. Lett.* **1996**, *77*, 3865 (Errata: *Phys. Rev. Lett.* **1997**, *78*, 1396).
(21) Zhang, Y.; Yang, W. *Phys. Rev. Lett.* **1998**, *80*, 890.
(22) Hammer, B.; Hansen, L. B.; Nørskov, J. K. *Phys. Rev. B* **1999**, *59*, 7413.
(23) Becke, A. D. *J. Chem. Phys.* **1988**, *88*, 1053.
(24) Becke, A. D.; Roussel, M. R. *Phys. Rev. A* **1989**, *39*, 3761.
(25) Becke, A. D. *J. Chem. Phys.* **1993**, *98*, 1372.
(26) Becke, A. D. *J. Chem. Phys.* **1993**, *98*, 5648.
(27) Stephens, P. J.; Devlin, F. J.; Chabalowski, C. F.; Frisch, M. J. *J. Phys. Chem.* **1994**, *98*, 11623.
(28) Scuseria, G. E. *J. Phys. Chem. A* **1999**, *103*, 4782.
(29) Goedecker, S. *Rev. Mod. Phys.* **1999**, *71*, 1085.
(30) Werner, H.-J., Manby, F. R., Knowles, P. J. *J. Chem. Phys.* **2003**, *118*, 8149.
(31) Schütz, M.; Manby, F. R. *Phys. Chem. Chem. Phys.* **2003**, *5*, 3349.
(32) Goedecker, S.; Scuseria, G. E. *Comput. Sci. Eng.* **2003**, *5* (4), 14.
(33) Mattsson, A. E. *Science* **2002**, *298*, 759.
(34) Tao, J.; Perdew, J. P.; Staroverov, V. N.; Scuseria, G. E. *Phys. Rev. Lett.* **2003**, *91*, 146401.
(35) Staroverov, V. N.; Scuseria, G. E.; Tao, J.; Perdew, J. P. *J. Chem. Phys.* **2003**, *119*, 12129.
(36) Fan, L.; Ziegler, T. *J. Chem. Phys.* **1990**, *92*, 3645.
(37) Fan, L.; Ziegler, T. *J. Am. Chem. Soc.* **1992**, *114*, 10890.
(38) Sosa, C.; Lee, C. *J. Chem. Phys.* **1993**, *98*, 8004.
(39) Andzelm, J.; Sosa, C.; Eades, R. A. *J. Phys. Chem.* **1993**, *97*, 4664.
(40) Stanton, R. V.; Merz, K. M., Jr. *J. Chem. Phys.* **1994**, *100*, 434.
(41) Porezag, D.; Pederson, M. R. *J. Chem. Phys.* **1995**, *102*, 9345.
(42) Truong, T. N.; Duncan, W. *J. Chem. Phys.* **1994**, *101*, 7408.
(43) Bell, R. L.; Truong, T. N. *J. Chem. Phys.* **1994**, *101*, 10442.
(44) Nguyen, M. T.; Creve, S.; Vanquickenborne, L. G. *J. Phys. Chem.* **1996**, *100*, 18422.
(45) Durant, J. L. *Chem. Phys. Lett.* **1996**, *256*, 595.
(46) Baker, J.; Muir, M.; Andzelm, J. *J. Chem. Phys.* **1995**, *102*, 2063.
(47) Baker, J.; Andzelm, J.; Muir, M.; Taylor, P. R. *Chem. Phys. Lett.* **1995**, *237*, 53.
(48) Jursic, B. S. *Chem. Phys. Lett.* **1995**, *244*, 263.
(49) Jursic, B. S. *J. Chem. Phys.* **1996**, *104*, 4151.
(50) Skokov, S.; Wheeler, R. A. *Chem. Phys. Lett.* **1997**, *271*, 251.
(51) Bernardi, F.; Bottoni, A. *J. Phys. Chem. A* **1997**, *101*, 1912.
(52) Lynch, B. J.; Fast, P. L.; Harris, M.; Truhlar, D. G. *J. Phys. Chem A* **2000**, *104*, 4811.
(53) Lynch, B. J.; Truhlar, D. G. *J. Phys. Chem. A* **2001**, *105*, 2936.
(54) Lynch, B. J.; Truhlar, D. G. *J. Phys. Chem. A* **2002**, *106*, 842.
(55) Lynch, B. J.; Truhlar, D. G. *J. Phys. Chem. A* **2003**, *107*, 8996 (Erratum: *J. Phys. Chem. A* **2004**, *108*, 1460).
(56) Zhao, Y.; Pu, J.; Lynch, B. J.; Truhlar, D. G. *Phys. Chem. Chem. Phys.* **2004**, *6*, 673.
(57) Kang, J. K.; Musgrave, C. B. *J. Chem. Phys.* **2001**, *115*, 11040.
(58) Hamprecht, F. A.; Cohen, A. J.; Tozer, D. J.; Handy, N. C. *J. Chem. Phys.* **1998**, *109*, 6264.
(59) Grant, D. M.; Wilson, P. J.; Tozer, D. J.; Althorpe, S. C. *Chem. Phys. Lett.* **2003**, *375*, 162.
(60) Wilson, P. J.; Bradley, T. J.; Tozer, D. J. *J. Chem. Phys.* **2001**, *115*, 9233.
(61) Van Voorhis, T.; Scuseria, G. E. *J. Chem. Phys.* **1998**, *109*, 400.
(62) Sadhukan, S.; Muños, D.; Adamo, C.; Scuseria, G. E. *Chem. Phys. Lett.* **1999**, *306*, 83.
(63) Proynov, E.; Chermette, H.; Salahub, D. R. *J. Chem. Phys.* **2000**, *113*, 10013.
(64) Filatov, M.; Thiel, W. *Chem. Phys. Lett.* **1998**, *295*, 467.
(65) Johnson, B. G.; Gonzales, C. A.; Gill, P. M. W.; Pople, J. A. *Chem. Phys. Lett.* **1994**, *221*, 100.
(66) Csonka, G. I.; Johnson, B. G. *Theor. Chem. Acc.* **1998**, *99*, 158.
(67) Patchkovskii, S.; Ziegler, T. *J. Chem. Phys.* **2002**, *116*, 7806.
(68) Jursic, B. S. *J. Chem. Soc., Perkin Trans. 2* **1997**, 637.
(69) Jursic, B. S. *J. Mol. Struct. (THEOCHEM)* **1998**, *427*, 157.
(70) Grüning, M.; Gritsenko, O. V.; Baerends, E. J. *J. Phys. Chem. A* **2004**, *108*, 4459.
(71) Pu, J.; Truhlar, D. G. *J. Chem. Phys.* **2002**, *116*, 1468.
(72) Baker, J.; Pulay, P. *J. Chem. Phys.* **2002**, *117*, 1441.
(73) Basch, H.; Hoz, S. *J. Phys. Chem. A* **1997**, *101*, 4416.
(74) Jursic, B. S. *Int. J. Quantum Chem.* **1997**, *62*, 639.
(75) Jursic, B. S. *J. Mol. Struct. (THEOCHEM)* **1998**, *434*, 53.
(76) Tozer, D. J.; Handy, N. C. *J. Phys. Chem. A* **1998**, *102*, 3162.
(77) Kobayashi, Y.; Kamiya, M.; Hirao, K. *Chem. Phys. Lett.* **2000**, *319*, 695.
(78) Barckholtz, C.; Barckholtz, T. A.; Hadad, C. M. *J. Phys. Chem A* **2001**, *105*, 140.
(79) Tokmakov, I. V.; Lin, M. C. *J. Phys. Chem. A* **2002**, *106*, 11309.
(80) Yeung, L. Y.; Elrod, M. J. *J. Phys. Chem. A* **2003**, *107*, 4470
(81) Jursic, B. S. *J. Mol. Struct. (THEOCHEM)* **1996**, *365*, 75.
(82) Barone, V.; Adamo, C. *J. Chem. Phys.* **1996**, *105*, 11007.
(83) Jursic, B. S. *J. Mol. Struct. (THEOCHEM)* **1998**, *428*, 49.
(84) Jursic, B. S. *J. Mol. Struct. (THEOCHEM)* **1998**, *428*, 55.
(85) Jursic, B. S. *J. Mol. Struct. (THEOCHEM)* **1998**, *430*, 17.
(86) Perdew, J. P.; Zunger, A. *Phys. Rev. B* **1981**, *23*, 5048.
(87) Goedecker, S.; Umrigar, C. J. *Phys. Rev. B* **1997**, *55*, 1765.
(88) Polo, V.; Kraka, E.; Cremer, D. *Mol. Phys.* **2002**, *100*, 1771.
(89) Gräfenstein, J.; Kraka, E.; Cremer, D. *J. Chem. Phys.* **2004**, *120*, 524.
(90) Gräfenstein, J.; Kraka, E.; Cremer, D. *Phys. Chem. Chem. Phys.* **2004**, *6*, 1096.
(91) Watanabe, N.; Kouchi, A. *Astrophys. J.* **2002**, *567*, 651.
(92) Crutcher, R. M. *Astrophys. J.* **1979**, *234*, 881.
(93) Harju, J.; Winnberg, A.; Wouterloot, J. G. A. *Astron. Astrophys.* **2000**, *353*, 1065.
(94) Woon, D. E. *J. Chem. Phys.* **1996**, *105*, 9921.
(95) Petraco, N. D. K.; Allen, W. D.; Schaefer, H. F., III. *J. Chem. Phys.* **2002**, *116*, 10229.
(96) Harding, L. B.; Wagner, A. F.; Bowman, J. M.; Schatz, G. C.; Christoffel, K. *J. Phys. Chem.* **1982**, *86*, 4312.
(97) Villà, J.; Corchado, J. C.; González-Lafont, A.; Lluch, J. M.; Truhlar, D. G. *J. Phys. Chem. A* **1999**, *103*, 5061.
(98) Harding, L. B.; Guadagnini, R.; Schatz, G. C. *J. Phys. Chem.* **1993**, *97*, 5472.
(99) Zhang, S.; Truong, T. N. *J. Chem. Phys.* **2000**, *113*, 6149.
(100) Tsuchiya, K.; Yamashita, K.; Miyoshi, A.; Matsui, H. *J. Phys. Chem.* **1996**, *100*, 17206.
(101) Shiina, H.; Oya, M.; Yamashita, K.; Miyoshi, A.; Matsui, H. *J. Phys. Chem.* **1996**, *100*, 2136.

(102) Huber, K. P.; Herzberg, G. *Molecular Spectra and Molecular Structure. IV. Constants of Diatomic Molecules*; Van Nostrand: New York, 1979.
(103) Baskin, C. P.; Bender, C. F.; Bauschlicher, C. W., Jr.; Schaefer, H. F., III. *J. Am. Chem. Soc.* **1974**, *96*, 2709.
(104) Yu, H.-G.; Muckerman, J. T.; Sears, T. J. *Chem. Phys. Lett.* **2001**, *349*, 547.
(105) Yang, M.; Zhang, D. H.; Collins, M. A.; Lee, S.-Y. *J. Chem. Phys.* **2001**, *115*, 174.
(106) Pople, J. A.; Head-Gordon, M.; Fox, D. J.; Raghavachari, K.; Curtiss, L. A. *J. Chem. Phys.* **1989**, *90*, 5622.
(107) Halkier, A.; Helgaker, T.; Jørgensen, P.; Klopper, W.; Koch, H.; Olsen, J.; Wilson, A. K. *Chem. Phys. Lett.* **1998**, *286*, 243.
(108) Dunning, T. H., Jr. *J. Chem. Phys.* **1989**, *90*, 1007.
(109) Kendall, R. A.; Dunning, T. H., Jr.; Harrison, R. J. *J. Chem. Phys.* **1992**, *96*, 6796.
(110) He, Y.; He, Z.; Cremer, D. *Chem. Phys. Lett.* **2000**, *317*, 535.
(111) Frisch, M. J.; Trucks, G. W.; Schlegel, H. B.; Scuseria, G. E.; Robb, M. A.; Cheeseman, J. R.; Montgomery, J. A., Jr.; Vreven, T.; Kudin, K. N.; Burant, J. C.; Millam, J. M.; Iyengar, S. S.; Tomasi, J.; Barone, V.; Mennucci, B.; Cossi, M.; Scalmani, G.; Rega, N.; Petersson, G. A.; Nakatsuji, H.; Hada, M.; Ehara, M.; Toyota, K.; Fukuda, R.; Hasegawa, J.; Ishida, M.; Nakajima, T.; Honda, Y.; Kitao, O.; Nakai, H.; Klene, M.; Li, X.; Knox, J. E.; Hratchian, H. P.; Cross, J. B.; Adamo, C.; Jaramillo, J.; Gomperts, R.; Stratmann, R. E.; Yazyev, O.; Austin, A. J.; Cammi, R.; Pomelli, C.; Ochterski, J. W.; Ayala, P. Y.; Morokuma, K.; Voth, G. A.; Salvador, P.; Dannenberg, J. J.; Zakrzewski, V. G.; Dapprich, S.; Daniels, A. D.; Strain, M. C.; Farkas, O.; Malick, D. K.; Rabuck, A. D.; Raghavachari, K.; Foresman, J. B.; Ortiz, J. V.; Cui, Q.; Baboul, A. G.; Clifford, S.; Cioslowski, J.; Stefanov, B. B.; Liu, G.; Liashenko, A.; Piskorz, P.; Komaromi, I.; Martin, R. L.; Fox, D. J.; Keith, T.; Al-Laham, M. A.; Peng, C. Y.; Nanayakkara, A.; Challacombe, M.; Gill, P. M. W.; Johnson, B.; Chen, W.; Wong, M. W.; Gonzalez, C.; Pople, J. A. *Gaussian 03*, Revision B.4; Gaussian, Inc., Pittsburgh, PA.; 2003.
(112) Tsuneda, T.; Suzumura, T.; Hirao, K. *J. Chem. Phys.* **1999**, *110*, 10664.
(113) Proynov, E. I.; Sirois, S.; Salahub, D. R. *Int. J. Quantum Chem.* **1997**, *64*, 427.
(114) Handy, N. C.; Cohen, A. J. *Mol. Phys.* **2001**, *99*, 403.
(115) Adamo, C.; Barone, V. *J. Chem. Phys.* **1998**, *108*, 664.
(116) Filatov, M.; Thiel, W. *Mol. Phys.* **1997**, *91*, 847.
(117) Boese, A. D.; Doltsinis, N. L.; Handy, N. C.; Sprik, M. L. *J. Chem. Phys.* **2000**, *112*, 1670.
(118) Boese, A. D.; Handy, N. C. *J. Chem. Phys.* **2001**, *114*, 5497.
(119) Krieger, J. B.; Chen, J.; Iafrate, G. J.; Savin, A. In *Electron Correlations and Materials Properties*; Gonis, A., Kioussis, N., Eds.; Plenum Press: New York, 1999.
(120) Perdew, J. P.; Kurth, S.; Zupan, A.; Blaha, P. *Phys. Rev. Lett.* **1999**, *82*, 2544 (Erratum: *Phys. Rev. Lett.* **1999**, *82*, 5179).
(121) Becke, A. D. *J. Chem. Phys.* **2000**, *112*, 4020.
(122) Becke, A. D. *J. Chem. Phys.* **1996**, *104*, 1040.
(123) Adamo, C.; Barone, V. *Chem. Phys. Lett.* **1998**, *298*, 113.
(124) Ernzerhof, M.; Scuseria, G. E. *J. Chem. Phys.* **1999**, *110*, 5029.
(125) Adamo, C.; Barone, V. *J. Chem. Phys.* **1999**, *110*, 6158.
(126) Becke, A. D. *J. Chem. Phys.* **1998**, *109*, 2092.
(127) Baerends, E. J.; Autschbach, J. A.; Bérces, A.; Bo, C.; Boerrigter, P. M.; Cavallo, L.; Chong, D. P.; Deng, L.; Dickson, R. M.; Ellis, D. E.; Fan, L.; Fischer, T. H.; Fonseca Guerra, C.; van Gisbergen, S. J. A.; Groeneveld, J. A.; Gritsenko, O. V.; Grüning, M.; Harris, F. E.; van den Hoek, P.; Jacobsen, H.; van Kessel, G.; Kootstra, F.; van Lenthe, E.; Osinga, V. P.; Patchkovskii, S.; Philipsen, P. H. T.; Post, D.; Pye, C. C.; Ravenek, W.; Ros, P.; Schipper, P. R. T.; Schreckenbach, G.; Snijders, J. G.; Sola, M.; Swart, M.; Swerhone, D.; te Velde, G.; Vernooijs, P.; Versluis, L.; Visser, O.; van Wezenbeek, E.; Wiesenekker, G.; Wolff, S. K.; Woo, T. K.; Ziegler T. *ADF2002.02 (development/modified)*; SCM, Theoretical Chemistry, Vrije Universiteit, Amsterdam, The Netherlands; 2002.
(128) Boese, A. D.; Martin, J. M. L.; Handy, N. C. *J. Chem. Phys.* **2003**, *119*, 3005.
(129) Lynch, B. J.; Zhao, Y.; Truhlar, D. G. *J. Phys. Chem. A* **2003**, *107*, 1384.
(130) Sobolewski, A. L.; Domcke, W. *Phys. Chem. Chem. Phys.* **2002**, *4*, 4.
(131) Sobolewski, A. L.; Domcke, W. *J. Phys. Chem. A* **2002**, *106*, 4158.
(132) Gritsenko, O. V.; Ensing, B.; Schipper, P. R. T.; Baerends, E. J. *J. Phys. Chem. A* **2000**, *104*, 8558.
(133) Grüning, M.; Gritsenko, O. V.; van Gisbergen, S. J. A., Baerends, E. J. *J. Phys. Chem. A* **2001**, *105*, 9211.
(134) Schipper, P. R. T.; Gritsenko, O. V.; Baerends, E. J. *J. Chem. Phys.* **1999**, *111*, 4056.
(135) Grüning, M. unpublished results, 2003.
(136) Tuma, C.; Boese, A. D.; Handy, N. C. *Phys. Chem. Chem. Phys.* **1999**, *1*, 3939.